Diese Arbeit wurde vorgelegt am
Lehr- und Forschungsgebiet Theorie der hybriden Systeme

Planung von Photovoltaik und Energiespeichern unter Berücksichtigung dynamischer Strompreise und Einspeisevergütung

Planning of photovoltaics and energy storage systems taking into account dynamic electricity and feed-in tariffs

Masterarbeit
Informatik

18. Juli 2024

Vorgelegt von Presented by	Jakob Dobmeier Matrikelnummer: 433600 jakob.dobmeier@rwth-aachen.de
Erstprüfer First examiner	Prof. Dr. rer. nat. Erika Ábrahám Lehr- und Forschungsgebiet: Theorie der hybriden Systeme RWTH Aachen University
Zweitprüfer Second examiner	Prof. Dr. Jürgen Giesl Lehr- und Forschungsgebiet: Software Analyse und Verifikation RWTH Aachen University
Betreuer Supervisor	Dr. rer. nat. Pascal Richter Lehr- und Forschungsgebiet: Theorie der hybriden Systeme RWTH Aachen University

Contents

1. Introduction

1.1. Motivation

Rising awareness and concerns about possible consequences caused by climate change encourage governments, researchers and industries to rapidly work towards a shift away from burning fossil fuels towards a sustainable energy system based on renewable energies [21]. For example Germany has put forth legislation aiming to close down its last coal-fired power plants no later than 2038 [16]. The transition from conventional power plants towards renewable energies requires more than simply replacing coal-fired power plants with hydroelectricity, solar and wind. The big advantage of traditional power generation is the controllability and consistency at which power can be generated. In comparison, power generated from wind or solar is volatile, dependent on the external uncontrollable conditions such as sufficiently strong wind or sunlight. Consequently, the timing of peak energy production may not align with the demand of the energy grid. To effectively utilize excess production and satisfy demand during periods of low generation, a form of energy storage is essential. There are various methods of energy storage available, including pumped hydro storage, batteries, and the conversion of excess energy into hydrogen or ammonium.

In the last 10 years the generation and storage of electricity from solar panels has become more and more affordable. Prices for lithium-ion battery packs have dropped from 780$/kWh in 2013 to 139$/kWh in 2023. This is a drop in prices by over 80%. Prices are projected to slowly decline further to 80$/kWh in 2030 [5]. During the same time period prices for solar panels have dropped by around 75% from 3629€/kWp in 2010 to 804€/kWp in 2020 [15]. In recent years there has been a shift away from feeding generated electricity into the grid towards self-consumption. The reason behind this trend is for one the low prices for battery storage capacity as well as the steadily declining feed-in tariffs (8.03 ct/kWh in October 2024) [6].

Two other sectors heavily reliant on fossil fuels are heating and mobility. An alternative to traditional heating using oil, wood or gas are heat pumps. Heat pumps use electricity to exchange heat from two separate system, i.e., inside the house and outdoors to either heat the building in winter or cool it in the summer. Current trends in personal mobility include replacing traditional cars with an electric vehicle (EV). The European Union aims to limit the first registration of new vehicles to those without CO2 emission by 2035. The usage of heat pumps and electric vehicles strongly increases the amount of annual consumed electricity. The combination of these large consumers with cheap electricity produced locally by PV is therefore an interesting topic for analysis.

The question how to design a system composed of PV, battery storage and (energy-intensive) consumers is itself non-trivial. It depends on various parameters such as geographical location, suitability of the roof, annual consumption or the size of the battery storage. In this thesis, we explore how to optimally design such a system. We integrate automated planning of photovoltaic (PV) installations tailored to specific roofs with a parameterized simulation of energy consumption and generation. We

include different scenarios and cutting-edge trends in PV and battery storage systems. This enables us to determine the optimal battery storage size, maximizing the self-consumption rate (SCR), which allows for a system that is both sustainable and economically feasible.

1.2. Related work

1.2.1. Estimation of roof area

The first step in any photovoltaic (PV) project is the careful identification of suitable project surfaces. This initial phase is crucial as it sets the foundation for the overall success of the installation. In the context of photovoltaics, there are two primary scenarios to consider: the installation of PV systems in open spaces, such as fields or bodies of water, and the installation on (residential) roofs.

Roofs in particular play a key role in urban areas for solar energy generation, primarily due to the limited availability of suitable open spaces. In densely populated environments, utilizing existing structures for PV installations is not only practical but also essential for maximizing solar energy production. Additionally, producing power where it is directly consumed reduces the need for expensive power grid infrastructure. Roofs, however, are not uniform. Instead they are often irregularly shaped, contain structural obstacles and different angles of slope. It poses a big challenge to correctly identify the roof surfaces that are suitable for PV installation.

Statistical estimation

Statistical approaches are used to estimate the solar energy potential on roof surface on a large scale such as entire cities or countries. Due to their statistical nature, these estimations only provide a rough estimate of the solar potential compared to more detailed, model-based approaches. Statistical approaches utilize parameters such as population density, land usage or the average footprint of buildings to estimate the roof surface available within the project area. For higher accuracy different zones, such as residential, commercial or industrial, are taken into account having different characteristics. An average usability coefficient depending on the roof type is used to estimate the area suitable for PV panel placement [8][22].

Image-based techniques

Image-based techniques perform well on segmentation tasks. The availability of high-resolution aerial and satellite imagery provides many different methods for the extraction of roof surfaces. Image-based techniques include:

Thresholding: Using a difference in the intensity/color of the pixel to distinguish roof area from non roof area [10][20][36]

Edge-recognition: Segment an image by identifying edges where certain properties sharply change

Clustering: Group pixels with similar properties together [1]

Deep-learning: (Convolutional) Neural networks are used to classify pixels in the image roof surface or non roof surface [28]

Digital surface model approaches

A digital surface model (DSM) is a highly detailed, three-dimensional digital representation of an object or surface such as a planet, city or building. Digital surface models are mostly created using high-resolution aerial or satellite imagery or advanced techniques such as Light Detection and Ranging (LiDAR). Depending on the resolution of the method used to create the DSM it can include only outline basic geometric shapes or even very intricate substructures.

The image-based techniques thresholding, edge-recognition, clustering or deep-learning can be adopted and work well on DSMs. Additional information such as height allows for augmented segementation of pixels belonging to the roof surface [2][3][28][20].

1.2.2. Obstacle detection

Obstacle detection plays an important role in improving the accuracy for estimation of solar potential. The existence of obstacles on a roof surface such as pipes, ladders, windows, chimneys, or dormers may cause the roof surface to be geometrically complex or segmented further. Simplified assumptions regarding the roof's complexity may cause a panel placement to be infeasible or suboptimal when applied in reality. A study done by Krapf et al. shows that insufficient obstacle recognition causes overestimations of up to 30% [26].

Large obstacles that strongly differ from the roof surface, such as chimneys or dormers, are often implicitly detected by classifying them as non-roof surfaces during roof surface extraction. Smaller obstacles however such as thin pipe are often overlooked due to the resolution of the images or DSM used. Planar obstacles such as windows or already existing PV panels may remain undetected due to similarity in slope, orientation and height [2][3][10][26][36].

Krapf et al. [26] provide a roof information dataset containing about 1800 manually labeled images of buildings of different classes of roof obstacles e.g. PV panels, windows dormers, and chimney. They demonstrate that using U-Net, a convolutional neural network known for its good performance on segmentation tasks, it is possible to classify even small obstacles.

1.2.3. Photovoltaic energy estimation

The amount of electrical energy produced by a solar panel depends on a multitude of different factors:

- **Irradiation:** The power produced is directly dependent on the amount of irradiation hitting the solar panel.

- **Slope:** The slope of the roof impacts at which angle solar rays hit the panel. This influences which fraction of the energy is convertible.
- **Orientation:** The orientation of the panel relative to the true solar south. Maximal energy can be harvested if the panel face true solar south at noon.
- **Temperature:** Deviating from the optimal temperature of 25°C reduces the efficiency of solar panels.
- **Minimal irradiation:** The lowest amount of irradiation received by any part of the solar panel determines the overall efficiency of the panel. If irradiation is to low for any part of the panel it will not produce any energy.
- **Debris:** Solar panels covered in dust, debris or snow have reduced efficiency due to reduced irradiation hitting the panel.
- **Shadowing:** Shadows of trees, surrounding building or superstructures on the roof reduce the amount of irradiation received by a (part of the) solar panel.
- **Area:** Increasing the area covered with solar panels directly increases the electricity produced.

In order to estimate photovoltaic potential, at a minimum the area covered by solar panels and the amount of radiation hitting them are required. For large scale analysis on a national or city level often only these two parameters are used [8][22][20].

The photovoltaic (PV) potential can be estimated more accurately by taking into account the slope and orientation of the panels. Both of these parameters impact the angle at which photons strike the surface of the panel and, therefore, how much energy can be absorbed and converted into electricity [2][3][10].

Shadowing not only decreases the amount of irradiation reaching the solar panel but may also cause panels to fall below the minimum irradiation threshold causing them to not produce any energy at all. Because solar panels in an array work in series it is important that no panel falls below this threshold since this would cause all panels in the series to stop producing energy [3][10].

Temperature and debris are usually not directly included in studies but integrated using a performance factor approximating the efficiency of the panel in a specified study area [2][3][10].

1.2.4. Solar panel placement algorithms

Maximum fitting grid placement

The method used by de Vries et al. [10] is simplistic. It works by overlaying a grid of vertically and horizontally aligned panels onto the roof surface and calculate the maximum number of panels fitting inside the roof surface. Panels intersecting with obstacles or reaching beyond the roof's borders are eliminated. By iteratively shifting

the grid along both length and width of the roof, with a fixed step size, all possible configurations of the grid are checked.

The limitations of this approach include failing to consider the amount of energy produced by each panel. The maximum amount of panels may not result in the optimal placement for maximum energy production. Additionally, not taking into account irradiation may cause panels to fall below the minimum irradiation threshold [2].

Integer linear programming

In their work Zhong et al. [36] solve the panel placement by formulating it as a special case of the *Maximal Covering Location Problem (MCLP)* called *Maximal PV Panel Coverage Problem (MPPCP)*. The goal of MCLP is to find the maximum amount of area coverable by placing a fixed number of facilities with a certain covering area. In MPPCP PV panels act as facilities covering the demand - roof surface to be covered - in a rectangular area around themselves. An additional restriction in the MPPCP compared to the traditional MCLP is that each area may only be covered by at most one facility. Using the commercial solver CPLEX they obtain an optimal panel placement for their problem formulation. The limitations of this approach were critiqued by Aslani and Seipel. According to them the modeling is insufficient due to placements being allowed to cross segment borders and not taking into account shadowing [2].

Genetic algorithms

Genetic algorithms are a meta-heuristic inspired by the principles of natural selection, gene crossover and mutation. Genetic algorithms drive the solution towards a desired outcome such as the maximization or minimization of a target function through natural selection of the best solutions in each iteration. Crossover allows for exchange or combination of properties between solution candidates to form new variants. Mutation introduces change into a candidate with a certain mutation probability. The aim of a genetic algorithm is to find a solution that satisfies a stopping criterion or to select the best solution found in a fixed number of iterations.

Aslani and Seipel [3] formulate an optimization problem maximizing the electricity generated by a solar panel layout. Their model restricts all panels in a certain layout to follow the same orientation. The rotation can be chosen arbitrarily for each layout. All panels are placed as close as possible without overlap starting from a point of origin. Panels are only placed if they fit onto the roof entirely and satisfy a minimal threshold of produced energy. The optimization problem is solved using a genetic algorithm starting on a population of randomized layouts. Since the maximization problem is solved individually for each separate continuous roof surface all panel layouts are near-optimal in their respective segment. A limitation of this approach is its fixed alignment of panels due to practical restrictions. Zhong and Tong [35] investigated the effect of panel alignment on optimal placement and suggested that allowing no-alignment can improve the coverage of roof surfaces.

1.2.5. Sizing of battery storage

There are two primary operational scenarios for battery storage systems. The first scenario involves integration with a power generation source, such as PV systems. In this configuration, battery storage functions as a buffer between energy generation and consumption, enabling users to utilize stored energy as needed, rather than being constrained to consume power only when it is produced. The second scenario focuses on grid-connected storage, where the battery is used in conjunction with a smart meter and a time-of-use (ToU) electricity pricing contract. This setup allows consumers to purchase electricity from the grid during periods of low prices and sell it back at a later time for a profit. Furthermore, a hybrid approach that combines both scenarios is a likely future trend with increasing advancements and implementation of a smart energy grid.

Self-consumption

In order to optimize a combined system of PV and battery storage several factors have to be taken into account. The produced energy directly depends on the installed capacities of the PV system. Furthermore, the offset between consumption period and times with power generation directly impacts the effectiveness and size requirements of the battery storage.

Boeckl and Kienberger [6] provide a greedy sizing method for battery storage based on the annual electricity requirement, size of the installed PV system and annual electricity consumption. They show that using a battery storage for self-consumption is economically viable assuming current prices for storage capacity and PV.

Stenzel et al. [33] highlight the importance of using realistic load profiles in order to accurately design a PV-battery storage system. Synthetic or aggregated load profiles may lead to over- or underestimation of required storage.

Hennings et al. [19] demonstrates how the degree of self-consumption changes significantly depending on the the household scenario used. Their work investigates how changes to the household such as taking in elders or kids leaving the household may impacts the system over its lifetime.

Beck et al. [4] provide a review of literature on the impact of temporal resolution when simulating PV-battery systems. They conclude that a temporal resolution of 15min is sufficient to achieve acceptable error rates of less than 5%.

Grid-connected storage

Dufo-López and Bernal-Agustín [11] analyzes the economic feasibility of using a grid connected storage for purchasing power at low prices and selling it back to the grid later with a profit. They assume a cost difference of 0.135€/kWh between high and low peaks. They conclude that it becomes profitable for lead acid battery storage once prices drop below 700€/kWh. Lithium-ion battery systems are profitable for prices of 300€/kWh and below.

Javeed et al. [23] use a particle swarm optimization algorithm in order to estimate optimal PV and battery storage size using flat and ToU pricing. They conclude that using ToU results in the best net present value.

Pan et al. [29] compare ToU and flat tariffs using a rule-based energy management system controlling the behavior of a fixed energy system consisting of PV, battery storage and consumers.

Sepúlveda-Mora and Hegedus [31] investigate the impact of combining PV and battery storage for commercial buildings. They use the HOMER grid software to simulate the energy production and consumption over a whole year using different load profiles with a temporal resolution of 15min. Parameters included in the simulation are battery degradation, different electricity pricing models and size of the PVs.

1.3. Contribution

This thesis contributes to the field in multiple points:

Discrete rooftop model: We provide a discrete rooftop model with with accurate modeling of regulations and practical restrictions for solar panel placements in Germany.

Placement algorithms: We develop optimal and heuristic algorithms solving the solar panel placement problem with constraints.

Energy system model: We build a parameterizable model of PV, battery storage, heating, electricity consumption and electric vehicle including their interaction.

Simulation of the energy system: We simulate the PV and battery storage system using a time-discrete deterministic simulation. This allows us to investigate the behavior of the system with reasonable precision and evaluate economic profit and sustainability.

Inclusion of current trends: In an effort to maximize sustainability we include the electrification of heating and personal transport by modeling the usage of a heat pump and electric vehicle. Additionally, we investigate how time-of-use tariffs and time-of-use feed-in impacts the economics and use of photovoltaic and battery storage system.

1.4. Outline of this work

The discrete rooftop model

Given a specific rooftop, we present a methodology for translating it into a discrete computational model. This model is designed to incorporate various influential factors, including the spatial variability of irradiance, the presence of obstacles as well as both regulatory constraints and practical limitations for panel installation and maintenance. Furthermore, the process of identifying all feasible locations where solar panels can be

placed is described. Lastly the calculation of the theoretical power potential for each solar panel are demonstrated and the abstractions done in the model explained.

Solar panel placement

Building upon the discrete rooftop model, we formulate an integer programming (IP) approach for the solar panel placement problem. Solving this IP we obtain a optimal solution for the panel placement with maximal energy potential. In addition to the exact solution method, we also develop a family of heuristic algorithms aimed to efficiently calculate panel placements while respecting additional constraints including panel orientation, panel alignment or symmetry.

Result and validation of solar panel placement

To evaluate the performance and practical applicability of the proposed algorithms, two representative case study buildings are selected and modeled in detail. For each building the optimal placement is calculated to serve as a benchmark to assess the heuristic algorithms against. The evaluation does not only focus on the quality of the solution, i.e. the energy potential, but how applicable they are in terms of aestheticism and ease of installation.

Modeling of the energy system

We develop a comprehensive model of an integrated energy system that includes photovoltaic generation, battery storage, and connected energy consumers (including heat-pump and electric vehicle). Different scenarios, such as different lifetime periods, dynamic time-of-use tariffs or usage of bidirectional charging, are modeled to investigate the impact of possible future trends on the energy system.

Simulation of the energy system

By employing a deterministic time-discrete simulation of the energy system with a temporal resolution of 15min we simulate the behavior of the energy systems under the different scenarios. The impact different scenarios have on the system are evaluated. Special focus lies on the fact how the optimal size of the battery storage changes with regards to economic profitability and sustainability.

2. Modeling of solar panel placement

In order to automatically and optimally place solar panels on the roof, a digital representation is required. In this section we provide a detailed overview of how the digital roof model is created, which constraints limit possible solar panel placements and how the energy generated by a solar panel is estimated.

2.1. Discretization of the roof surface

The surface of a roof can be represented as a collection of polygons specifying different parts and superstructures of the roof. Figure 1 shows an sample roof containing a simple dormer at the south-facing roof surface and a chimney in the north-facing side.

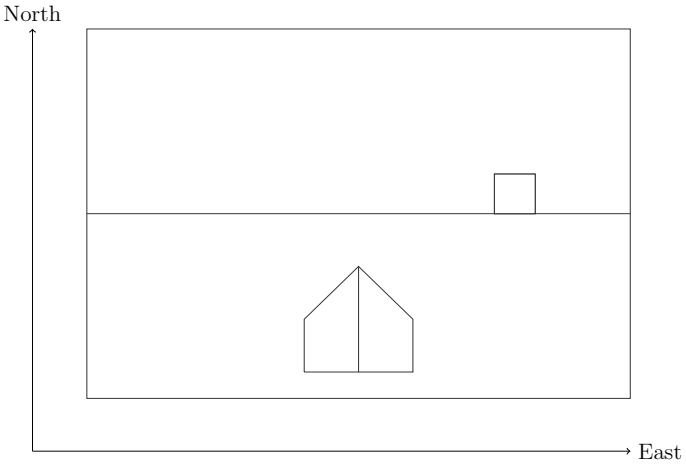

Figure 1: View of a roof from above. A chimney is located at the middle right of the roof and a dormer on the south facing roof.

A solar panel can be placed on every part of the roof that has sufficient space. This means the problem of photovoltaic placement is initially continuous. Continuous problems are difficult to model and solve [35]. In order to reduce the complexity of the problem, a common strategy is discretization. We use discrete steps of fixed size and split the roof into a finite grid of cells. Solar panels can now only be placed at these discrete steps, reducing the search space of feasible solutions to be bounded by the number of cells in the grid. Optimally, the step size is chosen such that the length of the solar panel and the size of the obstacles can be accurately represented. In our case this would mean to choose a size of 1mm due to wide variety of solar panel sizes available for modeling. This resolution is very high and again leads to a large search space for the placement optimization problem. In order to avoid this we initially start with a cell size of 10cm and increase the resolution up to 1cm if necessary to obtain accurate results. The error introduced by this modeling is analyzed and its impact discussed in details in Section 4.2.

2.2. Constraints

The usable surface for photovoltaics unfortunately does not simply coincide with the roof's surface but is restricted by multiple constraints. Obstacles present on the roof, building, fire safety regulations, as well as practical constraints limit the space actually suitable for a PV system. The result can in cases be a disconnected set of different (complex) polygons. In the following we will have a closer look at which constraints exist and how they are taken into account in our model.

Obstacles

Superstructures present on the roof hinder the installation of solar panels. Even small obstacles such as pipes or cables can in practice prevent panel installation. If obstacles are ignored this can cause an overestimation of up to 30% in the photovoltaic estimation [26]. All cells overlapping with obstacles identified on the roof are labeled as unsuitable and marked accordingly to exclude them from further consideration for panel placement and reduce their negative impact on solution quality.

Regulatory constraints

In most countries modifications to buildings have to comply with building regulations and fire safety regulations. We describe and model the regulations in place in Germany. Due to the federal system in Germany there is no national legislation but 16 different federal building and fire protection regulations. In some federal states such as Baden-Wuerttemberg, North-Rhine-Westphalia or Saxony-Anhalt there is no requirement for fire gaps between solar panels and neighboring buildings or on shared roofs. Other federal states require 50cm or 125cm gap depending on the local legislation. Additionally some federal states have different regulations depending on whether the solar panel is classified as easily burnable or not. Lastly, all federal states have in common that they do not require a fire gap to the neighbor if there is a fire wall with a height of at least 30cm separating neighboring roofs. A full overview of this can be seen in Appendix A.

Due to this complexity the different buffer zones are modeled as configurable parameters depending on the applicable regulations. This decision ensures the extensibility of the model for changing regulations or different countries.

Practical constraints

In addition to governmental regulations there are practical constraints hindering the installation of solar panels. On the edge of the roof wind and snow exert greater force on the solar panels. Therefore in practice a boundary of 30-40cm is left unused in order to avoid damage to panels or prevent them from being torn off the roof.

The placement of solar panels on tiled roofs uses an substructure placed beneath the roof tiles. Due to this construction in practice there is a gap remaining at the ridge of the roof of a half tile. For a standard roofing tile of 30cm this is a gap of 15cm. The same holds true for the bottom eave.

Although, there is no regulation requiring solar panels to keep a distance from roof superstructures, such as chimneys or windows, usually an area of 15-20cm is left unused. First, this is a practical reason allowing for easier installation and maintenance of the panels. Second, areas close to obstacles are more likely to experience shadowing and therefore not as well suited for solar panels.

All these constraints are also modeled as parameters to allow for precise configuration and to account for possible future changes.

2.3. Extraction of suitable roof area

Given a roof such as shown in Figure 2 we classify each cell into one of the following four categories: roof surface, obstacle, buffer and non-roof. Buffer zones and obstacles are located on the roof but limit the installation capacities for PV. Only areas not overlapping with buffers or obstacles are usable.

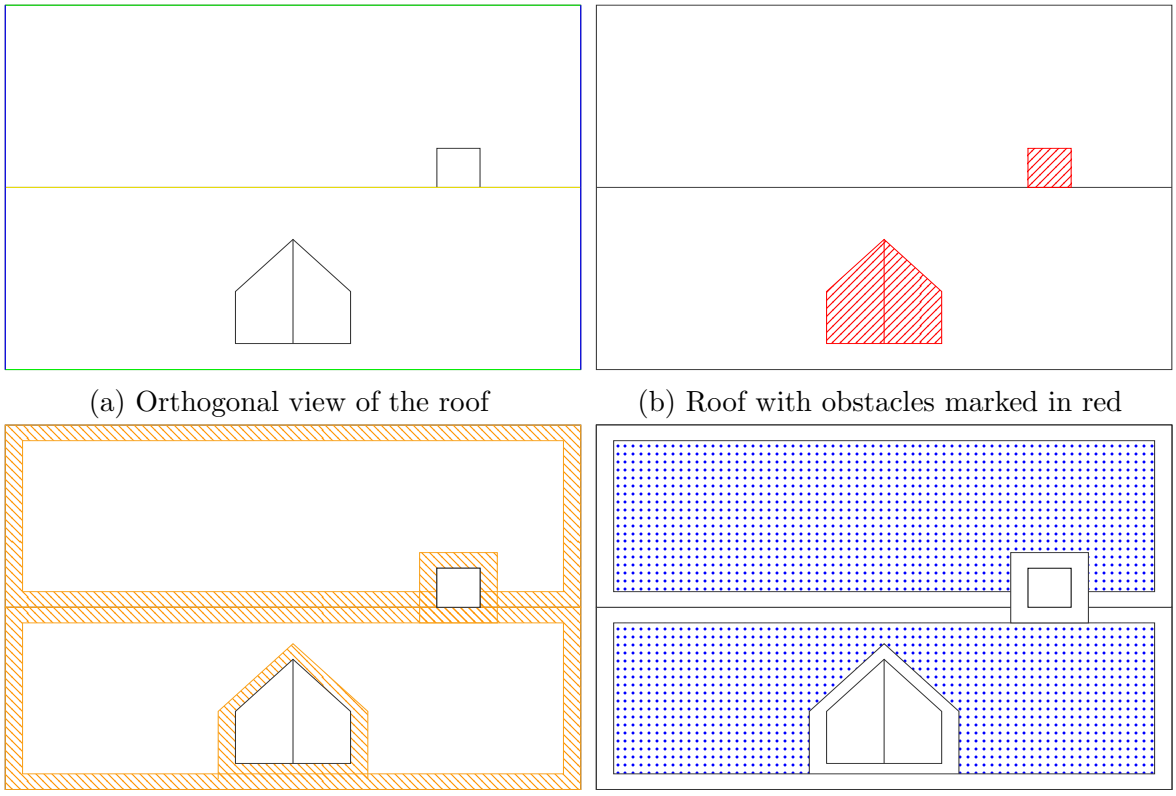

(a) Orthogonal view of the roof

(b) Roof with obstacles marked in red

(c) Roof with bufferzone marked in orange.

(d) Roof area suitable for PV in blue.

Figure 2: Extraction of roof surface suitable for PV installation. Removing obstacles and buffer zones for more accurate PV estimation. The edges of the roof colored in (a) represent rakes (blue), eaves (green) and ridge (yellow). Shadowing is included by declaring buffer zones around the obstacles.

Obstacles

The roof and obstacles are both obtained as input data. Parts of the roof overlapping with obstacles are marked accordingly. Allowing to treat them accordingly in further processing, i.e. with regard to placing solar panels. Figure 2b depicts the elimination of obstacles by marking them on the roof. This method requires precise labeling of the input data.

Buffers

As discussed in Section 2.2 regulations and practical constraints limit the placement of solar panels on the roof. We model these constraints using buffer zones. Buffers are variable-sized back-offs depending on the type of buffer, e.g. edge buffer or obstacle buffer. In order to find these buffer zones we first classify all cells with similar orientation and slope as a homogeneous roof segment. Secondly, edge detection is employed to find all cells which are located at these edges (e.g. roof edge, roof peak, or next to obstacles). From these cells the respective buffer space is expanded and all cells located within it marked accordingly. In Figure 2c two roof faces - north and south - are identified and their buffers removed.

Roof and non-roof cells

Non-roof serves as a catch-all for any part of the input that is neither buffer, obstacle or roof surface. This allows us to model roof with complex polygonal shape easily by assigning areas labeling areas outside of the roof surface as *non-roof*.

After removing obstacles and buffer zones, all remaining cells with the label *roof* are considered preliminary candidates for solar panel placement. Each of these candidates will be further investigated for suitability as discussed in Section 2.6.

2.4. Photovoltaic panel modeling

To accurately model the behavior of PV panels it is key to understand the basic operation principles. A panel consists of smaller photovoltaic cells which are fabricated from photovoltaic material - most commonly crystallized silicone wafers. When enough solar irradiation strikes a cell a small amount of electricity is generated. In order to generate high enough voltage the cells are connected in a series - so called ”strips”. In a series circuit the voltages of the individual components add up whilst the current is equal in all components.

$$U_{Strip} = \sum_{c \in Cells} U_c \qquad\qquad I_{Strip} = I_c \; \forall c \in Cells$$

Multiple of these strips are then installed in parallel in order to amplify the current I_{Panel} to a desired level. In a parallel circuit the currents of the components add up and the voltages are equal for every component.

$$U_{Panel} = U_s \; \forall s \in Strips \qquad\qquad I_{Panel} = \sum_{s \in Strips} I_s$$

A series circuit has the downside that the current has to flow through each connected cell sequentially. A malfunctioning or shadowed cell could therefore lead to the whole strip not producing any electricity - so called "Christmas light effect". In order to avoid this every cell is paired in parallel with a bypass-diode allowing current to flow around a non generating cell. This means that the electricity generated by the whole solar panel is the sum of the electricity produced by each individual the photovoltaic cell. Since we can assume that each cell is identical this mean the amount of electricity produced is directly dependent on the sum of irradiation hitting the solar panel.

The amount of energy harvested by an solar panel depends not only on the conditions but on the characteristics of the solar panel as well. We will demonstrate which characteristics are taken into account at the example of the Trina Vertex S+ panel (see Fig. 3), which was one of the most used panels in Germany in 2023.

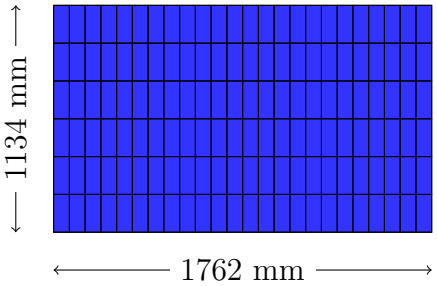

STC peak power	$P_{max} =$	425 W_{peak}
Temperature coefficient	$\beta_T =$	-0.29 %/°C
Efficiency	$\eta_{STC} =$	22.5 %
NOCT	$T_{NOCT} =$	43 °C

Figure 3: Representation of the the important key figures of a solar panel using the example of the model Trina Vertex S+.

The performance of a solar panel is measured under *Standard Test Conditions* (STC). The STC is fixed at an irradiance of 1000 W/m^2, an spectra of 1.5 air mass and a temperature of 25 °C. P_{max} is the nominal peak power produced at STC and measured in W_{peak}. The temperature coefficient β_T describes how the performance loss in % for each °C the cell temperature deviates from STC. The efficiency η_{STC} describes the ration of energy convertible from irradiance at STC in %. Furthermore the amount of irradiance convertible is directly proportional to the surface area of the panel.

2.5. Energy calculation

Theory

In theory a solar panel can reach efficiency values of up to 33.16%. In practice this value is much lower and usually around the $22 - 23\%$ range. Since the efficiency of panels is relatively low even small increases compound to a relatively big increase in

overall power generation over all panels and time. The actual efficiency of a solar panel can be calculated as shown in Eq. 1.

$$\eta = \eta_{STC} - \beta_T(T_c - T_{STC})) \tag{1}$$

$\eta :=$ Efficiency of the solar panel [%]
$\eta_{STC} :=$ Efficiency of the solar panel at STC [%]
$\beta_T :=$ Temperature coefficient from peak [%/°C]
$T_c :=$ Current temperature of the panel/cell [°C]
$T_{STC} :=$ Temperature at STC [°C]

The formula shows that the efficiency depends on the actual cell temperature T_c, the optimal panel efficiency at STC η_{STC} and temperature coefficient β_T. It describes the factor with which the efficiency of the panel decreases per degree Celsius deviation from the STC.

$$T_c = T_a + (\frac{I_{eff}}{800}) \cdot (NOCT - 20) \tag{2}$$

$T_a =$ Ambient temperature
$I_{eff} =$ Effective irradiance
$NOCT =$ Nominal operating cell temperature

The cell temperature can be estimated using the model described in Eq. 2. The base temperature equals the ambient temperature and is further increased by the absorption of irradiance.

$$E_a = A \cdot I_a \cdot \eta \cdot \gamma_{PR} \tag{3}$$

$E_a :=$ Annual energy produced [Wh]
$A :=$ Area [m^2]
$I_a :=$ Annual Irradiation
$\eta :=$ Efficiency of the solar panel [%]
$\gamma_{PR} :=$ Performance ratio of the solar panel [%]

The energy of a solar panel installation is usually computed using the formula provided in Eq. 3 and is widely used in different studies [3][28][36]. The performance ration γ_{PR} is a combined factor describing the energy lost by sub-optimal conditions in reality e.g. inverter loss or dirty panels. This factor is heavily dependent on the installation and usually approximated using the theoretical value of 80%.

Model

In order to estimate the quality of an panel placement we use the maximal energy generated as the deciding factor. Because all panels are installed on the same roof the conditions such as temperature or performance ratio can be assumed to be equal. Since additionally all solar panels installed have the same area the deciding factor for an optimal placement is the amount of irradiance collected among all panels placed. For simpler calculations we assume the panel to operate in optimal conditions therefore the efficiency of the panel is η_{STC} as this does not impact the comparability. For the Tirna Vertex S+ this is 22.5%. Furthermore we fix the performance ratio to the theoretical value of 80% since it too can be assumed to be the same for all panels in the installation.
In total we calculate the energy of a solar panel for optimal placement using an adapted version of Eq. 3 described in Eq. 4.

$$E_a = A \cdot I_a \cdot \eta_{STC} \cdot 0.8 \tag{4}$$

$$\begin{aligned} E_a &:= \text{Annual energy produced by a panel [Wh]} \\ A &:= \text{Area of the solar panel } [m^2] \\ I_a &:= \text{Annual irradiation} \\ \eta_{STC} &:= \text{Efficiency of the solar panel at STC [\%]} \end{aligned}$$

2.6. Identification of panel candidates sites in the grid

In order to place a solar panel on the discrete roof grid we define a so-called anchor point (AP) - upper-left corner of the solar panel in grid orientation - for each cell of the grid. For each pair of position and panel orientation - vertical or horizontal - on the grid it is checked whether a solar panel can fit and how much energy it would produce. A panel can fit on the grid it does not cross the roof edge and does not overlap with any buffer or obstacle. If a possible panel placement does not meet a minimum energy threshold it is discarded as inefficient. As a result we obtain a list of all possible panel anchor points on the roof.

2.7. Solar placement roof model

The roof model defined in this section contains a segmentation of the roof into distinct discrete surfaces. For each segment a collection of possible solar panel anchor points is known as well as obstacles, buffer zone and map of irradiance values. Figure 4 depicts visualization of the roof model consisting of a north and a south facing segment. Obstacles and buffer zones are excluded. Blue dots represent where both a vertically and a horizontally placed panels could be installed. Red/green dots represent only horizontal/vertical panels. The north facing segment does not contain any panel can-

didates even though enough space is available since due to low irradiance resulting in insufficient power generation.

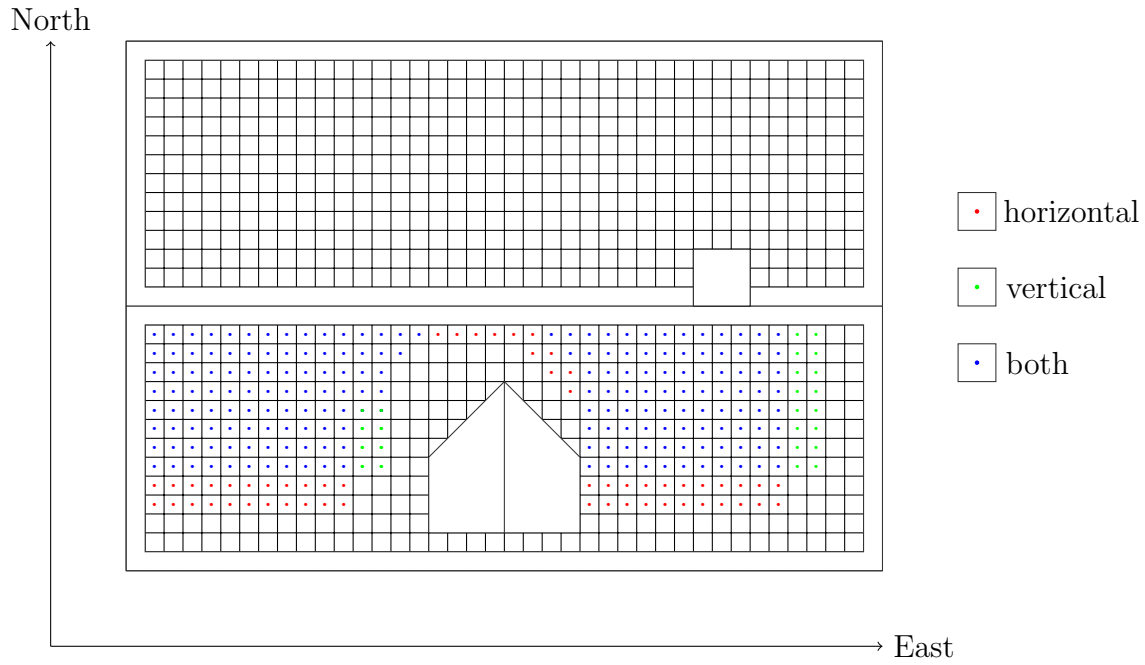

Figure 4: View of the roof with candidate anchor points for solar panel placement with a panel size of 5×3 cells. Buffer size for obstacles is 0 cells. Buffer size for segment edges are 1 cell.

3. Solar panel placement

This section focuses on the algorithms used to determine different possible panel placements. We develop three types of algorithms: an integer program yielding an exact solution, a mixed-alignment greedy algorithm and a grid-alignment algorithm. In the following we discuss how each of these algorithms work in more detail.

3.1. Integer Program

In their work Zhong et al. [36] develop a integer program maximizing the energy produced by the panels placed on the roof. We base an integer program - in the following referred to as *IP* - on their work and improve their construction by implementing improved pre-processing of suitable candidates (see Section 2) and adapt it to our model. The resulting integer program looks as follows:

$$\text{Maximize} \quad \sum_{o \in O} \sum_{i \in I} \sum_{j \in J} P_{ijo} \cdot X_{ijo} \tag{5}$$

subject to

$$\sum_{m=max(1,i-p_l)}^{i} \sum_{n=max(1,j-p_w)}^{j} X_{mnh} + \sum_{m=max(1,i-p_w)}^{i} \sum_{n=max(1,j-p_l)}^{j} X_{mnv} \leq 1 \qquad \forall i,j \tag{6}$$

$$X_{ijo} \in \{0,1\} \qquad \text{if } (i,j,o) \in C \tag{7}$$

$$X_{ijo} = 0 \qquad \text{if } (i,j,o) \notin C \tag{8}$$

$$I = \{1, ..., width\} \tag{9}$$

$$J = \{1, ..., height\} \tag{10}$$

$$O = \{v, h\} \tag{11}$$

$$C := \text{Candidate anchor points} \tag{12}$$

$$p_w := \text{Width of the solar panel} \tag{13}$$

$$p_l := \text{Length of the solar panel} \tag{14}$$

Eq. (5) ensures that we select the panel configuration with the maximal energy yield by summing the potential of each placed panel. Eq. (6) ensures that each cell is only covered by at most one solar panel meaning that no two solar panels overlap. Each candidate is a 3-tuple (i, j, o) with $i \in I, j \in J$ and $o \in O$ meaning a position of the grid and an horizontal or vertical orientation of the panel. p_w and p_l are the width and length of the solar panel as a whole number multiple of cells. The solution of the IP i.e. all $X_{ijo} = 1$ are a valid set of anchor points defining an optimal placement on the roof segment with maximal annual expected energy.

3.2. Greedy meta-heuristic

Integer programs can be slow to solve. For many problems a greedy algorithm yields good results with low computational effort. Our algorithm is a meta-heuristic - in the following referred to as *Greedy meta-heuristic* - selecting the best result out of two runs of the same greedy algorithm using different parameters. In the first run all possible panels with horizontal orientation are placed on the roof before placing vertically oriented panels. In the second run the order is reversed - vertical before horizontal orientation.

The greedy algorithm starts at the origin of the roof segment and traverses it first in width-wise and then in a height-wise order. If a panel can be anchored at the current cell the position and orientation are saved and an occupation mask for the segment is updated to avoid overlapping panels.

3.3. Aligned algorithms

Both the integer program and the greedy meta-heuristic allow for panels to be placed without taking into account the alignment of the panels. Even though this is no requirement for a valid placement alignment of the panels is a crucial factor for installation. Complex panel layouts increase the amount of manual labor needed for placing and correctly wiring the panels therefore increasing the overall cost of the installation significantly due to high cost of labor.

The alignment algorithms *Vertical* and *Horizontal* only allows for the usage of a single panel orientation within a roof segment in order to ensure alignment along both the short and long edge of the panel. The solar panel configuration with the highest annual energy output is determined by overlay a fully aligned grid of solar panels with the roof segment. In a second step it is shifted by all possible positions along the x and y-axis. Each position if evaluated and saved if it is maximal [10].

3.4. Symmetrical aligned algorithms

There exist a costumer group that heavily prioritizes aesthetics over maximizing the electricity generated from the photovoltaic installation. Mainly this aesthetic is with regard to alignment and the symmetry of solar panel placement. The alignment is already covered by the *Vertical* and *Horizontal* algorithms. Symmetry can be achieved by either aligning the panels along the vertical or horizontal bisecting line. In order to evaluate the impact of including the symmetry into the placement results the algorithms *Vertical* and *Horizonal* are adapted to *VerticalSym* and *HorizontalSym*. The expected result is a decline in placement quality but it is still interesting to evaluate how large the impact of this additional constraint is.

4. Results of solar panel placement

4.1. Case study objects

To evaluate the performance, quality and accuracy of our algorithms we take a look at two different houses. Figure 5 shows the two different case study objects. The house

Figure 5: Left is the first case study object consisting of roof with 4 segments low slope angle and a few, small chimney obstacles. Right is the second case study object. A semi-detached house with two roof segments, a dormer, chimney and a large window. Both houses are shown being oriented such that north is up. (Souce: GoogleEarth)

on the left side has relatively low slope, only some small- or medium-sized chimneys and is divided into four distinct roof segments. The second case study object, visible on the right, is one half of a semi-detached house. The roof consists of two large segments. The south-facing segment contains a large dormer whilst the north-facing one includes a large window aligned with the slope of the roof. The slope of the first roof was estimated to be 22° and for the second one, a slope of 30° was chosen.

4.2. Discretization error

The process of discretization introduces some error in our modeling. Every continuous value in our model has to be represented as a whole multiple of the discrete cell size chosen. If chosen well this does not introduce any error, i.e. if the cell size is a divisor of the cell size. Unfortunately solar panels and roofs appear in countless different sizes and shapes. In order to accurately represent this with discrete steps very small values, such as 1mm, would need to be chosen. This in turn again causes significant computational effort. We therefore have to expect that some error will be introduced by using reasonably large discrete values.

A continuous length l_{cont} is transformed into a multiple n of discrete cells with length c by rounding up the next whole multiple. This guarantees that every buffer, obstacle or panel described in the model actually fits and does not overlap. In the worst case $l_{cont} = n \cdot c + \varepsilon$ for a small $\varepsilon \geq 0$. Then the error introduced is $c - \varepsilon$ absolute.

Let us assume a cell size of $c = 0.1$m and the commonly used solar panel described in Figure 3 with dimensions 1.762m×1.134m. The error introduced for each solar panel is maximal along the short side of $l_{cont} = 1.134\text{m} = 11 \cdot 0.1\text{m} + 0.034\text{m}$. The absolute value of the error is $c - \varepsilon = 0.1\text{m} - 0.034\text{m} = 0.066\text{m}$. In order for the model to be inaccurate the error has to compound up to at least 1.134m. This only occurs if $\left\lceil \frac{l_{cont}}{c-\varepsilon} \right\rceil = \left\lceil \frac{1.134}{0.066} \right\rceil = 18$ panels can be placed continuously with a length of 20.412m. If we reduce the cell size to $c = 0.05$m the amount of panels required for a large enough compounding error increases to 71 panels or 80.514m. We assume that this is sufficient to cover most non-commercial rooftop PV systems and therefore suggest a cell size of 5cm.

4.3. Comparison of the placement layout

The quality of placements for practical use varies noticeably across the different algorithms. This is to be expected as the algorithms are designed to optimize focusing on different criteria e.g. energy, alignment or maximum roof-coverage.

The placement produced by the *IP* aims to maximize the annually generated energy. As can be seen in Figure 6a the placement does not posses any inherent regularity or order. In practice this placement would be very hard to install and the increased installation cost - which accounts for a large part of the overall cost - would most likely be economically infeasible and difficult to maintain.

The *Greedy meta-heuristic* aims to maximize the area of the roof coverage by solar panels. Due to this procedure locally aligned panel areas with the same orientation often emerge naturally whilst on other parts very little order emerges. This can be seen in 6b. On the left side the panels are almost vertically aligned. On the half of the roof segment panels appear less ordered and in mixed orientation.

The aligned algorithms *Vertical* and *Horizontal* both greatly restrict the flexibility of panel placements to a fixed grid of panels in either portrait or landscape orientation. This reduces the number of panels placed on the roof segment but guarantees the optimal installation conditions. Since the algorithm evaluates all possible grids on the roof surface it ensures that one of these placements is optimal given this strong alignment.

The addition of symmetry works well for roof segments that have inherent symmetry. For the south facing roof segment of Case Study 2 this is not the case. As Figure 6e and 6f show the panels are symmetrically aligned along the roof's vertical centerline reduces the number of panels and does nothing or only little to improve aesthetic appearance for this roof segment.

4.4. Comparison of the placement efficiency

The most important key figure for a PV system is the amount of power harvested from solar irradiance [36]. The placement generated as a solution for the *IP* is optimal for the model since it generates a valid placement and maximizes the amount of energy produced. In Figure 7 we can observe that with increasing restrictiveness of the algorithms, i.e. alignment and symmetry, the amount of panels and power generated decrease for both case studies. This is to be expected since with additional constraints no new solutions are generated but the number of feasible solutions is restricted.

In Figure 7 we can observe an improvement in panel count for all algorithms by increasing the grid resolution from 10cm to 5cm. This jump can be explained by additional space being freed up by (i) lower discretization error for the panels and (ii) no discretization error for chosen buffer sizes. As shown in Section 4.2 the error of the discrete model is dependent on the cell size. Thus additional possible roof area is freed up by using a smaller cell size. Additionally, since all buffer sizes are multiples of the cell size 5cm no error is caused by the buffer zones. Both of these factors combined provide enough additional space to allow for the placement of further panels. Another doubling of the grid resolution does not improve the panel count since only the discretization error for the panels decreases but insufficient space is freed up to allow for additional panel placement.

It is important to stress that this break-point is highly dependent on the roof simulated. However as we have discussed it is advantageous to select the buffer sizes as multiples of the cell-size (or vice-versa) and use lower cell size to reduce the discretization error overall. This enables us to achieve placements which possess a high degree of realism.

4.5. Runtime analysis

All runtime measurement were executed on a Thinkpad T570 using a Intel Core i5-7300U, 8GB DDR4 RAM and a Samsung Electronics NVMe PM981 1TB SSD. The operating system used was ManjaroLinux 25.0. All code was written in Rust using the compiler version 1.81.0.

The size of the discrete grid depends linearly on both the width W and length L of the roof segment. Furthermore the identification of valid candidates depends on the cell size c with $\mathcal{O}\left(\frac{1}{c^4}\right)$. This is due to the fact that the cell size for increases the number of cell both for length and width. The size of the grid therefore grows in $\mathcal{O}\left(\frac{W \cdot L}{c^2}\right)$. Secondly the number of cells which need to be checked for each panel to ensure it can be placed too grows in $\mathcal{O}\left(\frac{L_p \cdot W_p}{c^2}\right)$, with W_p and L_p being width and length of the solar panel. In total the runtime for candidate identification results in $\mathcal{O}\left(\frac{W \cdot L \cdot W_p \cdot L_p}{c^4}\right)$.

The heuristic algorithms themselves have only check each grid cell for validity at most once and therefore have all have runtime complexity in $\mathcal{O}\left(\frac{W \cdot L}{c^2}\right)$.

Since candidate identification is used as the basis for all algorithms and it's large runtime cost, all heuristic algorithms perform quite similarly overall as can be seen in

Figure 7. For cell sizes of 5cm or large the performance of the algorithms is acceptable with a runtime of at most 8.7s for Case Study 1 and 4.4s for Case Study 2.

Using parallelization and improving candidate identification are promising fields to reduce the runtime of all algorithms.

4.6. Discussion

The *IP* optimally solves the model and calculates a placement which achieves maximum energy output. However the layout of the placement calculated is not practically feasible for a real-world installation due to high degree of irregularity in the layout. Additionally, solving the problem is computationally too expensive. Therefore it is necessary to use heuristic algorithms if time is a limiting factor or the cell size is sufficiently small.

All heuristic algorithms perform reasonably well and provide satisfactory placements under different constraints. The *Greedy meta-heuristic* performs the best for maximizing energy and panel count since it possesses the least amount of constraints. Even though locally areas of aligned panels emerge no guarantees can be made regarding ease of installation.

The aligned algorithms *Vertical* and *Horizontal* provide aligned solar panel placements and are well suited for placements easily implementable in practice. Adding symmetry as an additional constraint may provide more aesthetically pleasing placements depending on the roof segment but requires inherent symmetry in the roof to work well.

We recommend using either *Greedy meta-heuristic* or *Vertical*/*Horizontal* to achieve the best results.

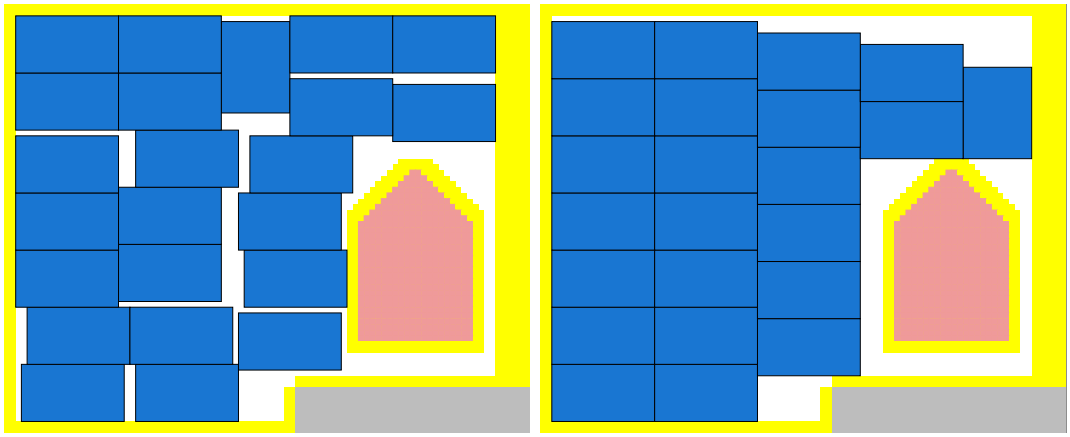

(a) IP [23]

(b) Greedy meta-heuristic [23]

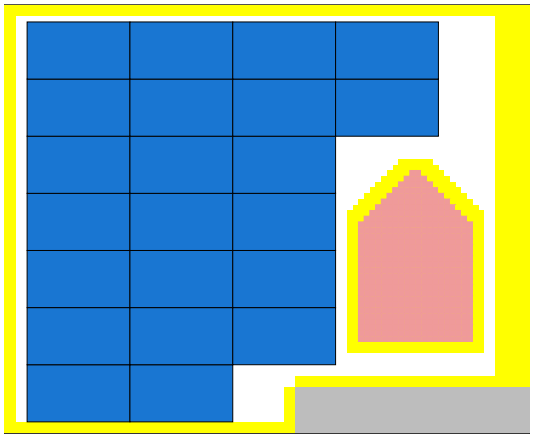

(c) Horizontal [22]

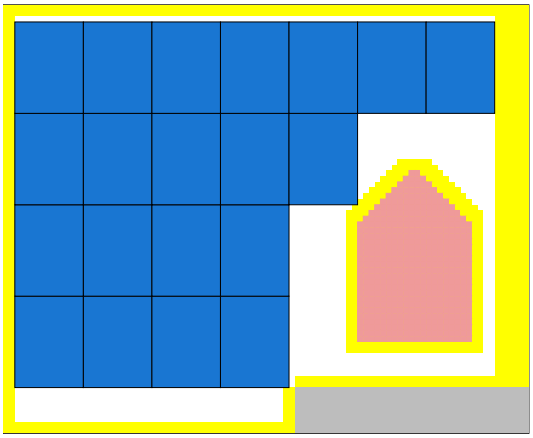

(d) Vertical [18]

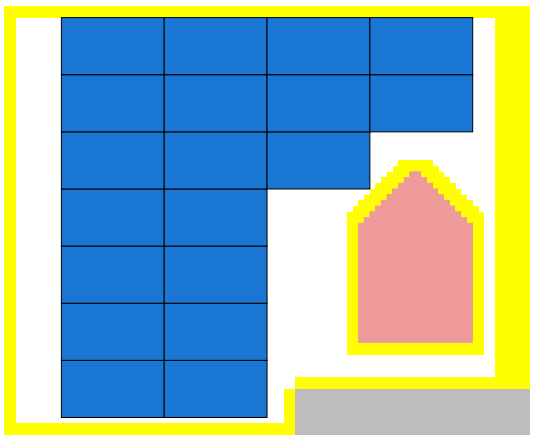

(e) HorizontalSym [19]

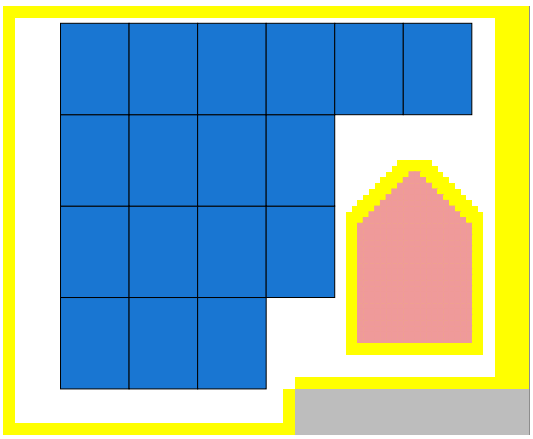

(f) VerticalSym [17]

Figure 6: Comparison of placements generated by the different algorithms on the south facing roof segment of Case Study two for a cell size of 10cm. Photovoltaic panels are shown in blue, obstacles in red and buffer zones in yellow. Unused roof surface remains white. The number of panels placed by each algorithm is given in the brackets

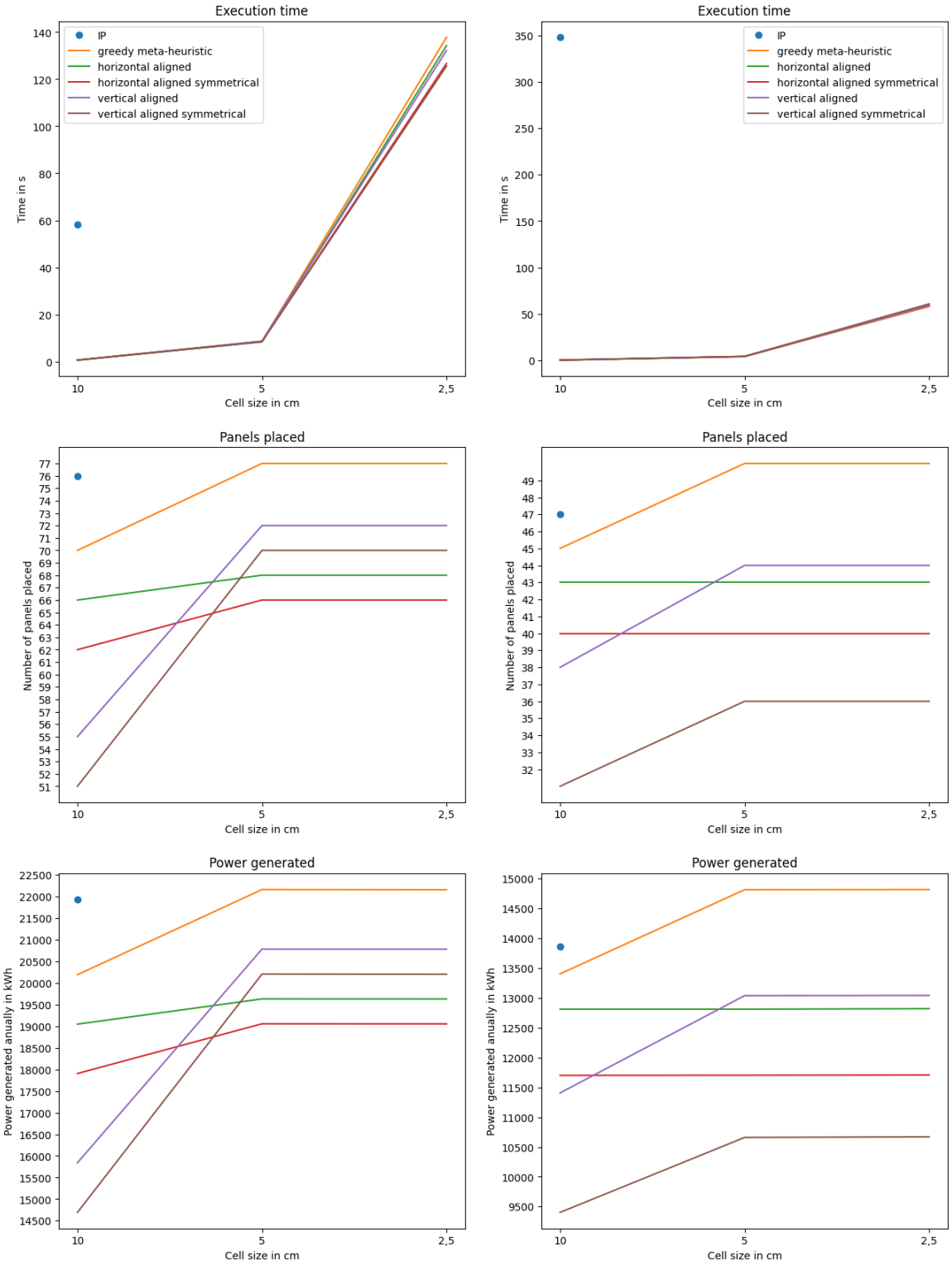

Figure 7: Evaluation of the two different Case Study objects with left being Case Study one and right Case Study two. Each algorithm was run with 10cm, 5cm and 2.5cm. For each object the execution time, number of panels placed and the power generated was analyzed.

5. Modeling of energy storage systems

Photovoltaic systems produce energy regardless of whether there is a demand for the electricity or not. Therefore, periods of over- and underproduction occur. There are different approaches on how to deal with this asynchronicity. One option is to sell the electricity to the grid for a fixed compensation. This approach is further detailed in Section 5.2. Another option is to use a energy storage system ,e.g. a battery, to buffer excess generation and provide power during periods of high consumption. Due to the low cost of self-generated electricity in comparison with purchasing it this can be economically profitable. In the following section we model an energy storage system consisting of consumers, photovoltaic power generators and energy storage units. We include current trends towards increased autarky (degree of self-sufficiency) and ecological friendliness. These include heating with heat-pumps instead of burning fossil fuels (see 5.4), dynamic feed-in and electricity tariffs (see Section 5.2 and Section 5.1) and using an electric vehicle battery as additional storage (see Section 5.8).

5.1. Modeling of electricity tariffs

For private customer, there are two different options for electricity tariffs: static tariffs and time-of-use (ToU) tariffs. As the name suggests static tariffs bill a fixed price for each kWh consumed, along with a fixed monthly base fee. For 2024 the average price was 39.5ct/kWh [13].

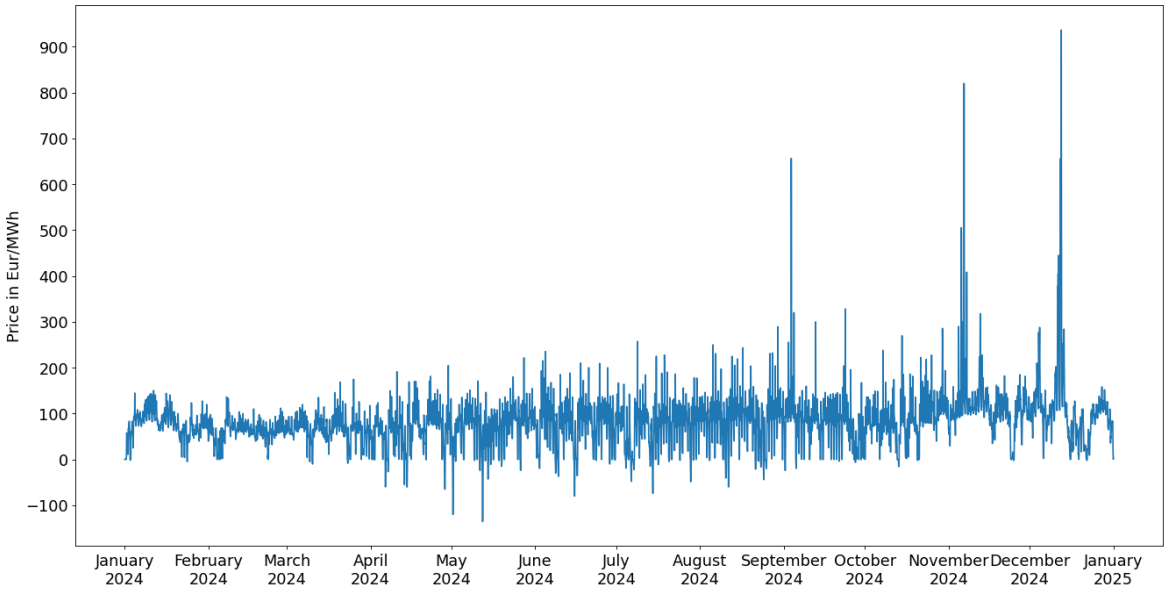

Figure 8: Spot market electricity prices in €/MWh for every hour in 2024. (Data provided by Energy-Charts.info [12])

The second option sets the price the kilowatt-hour price based on the time of use. In the past these were often just split segments of high and low demand e.g. daytime and

nighttime. Modern tariffs offer customers the freedom to directly purchase power at the price traded at the electricity price exchange. The day-ahead market negotiates, using auctions, how much a unit of power costs based on predictions of energy production and demand for the upcoming day between providers and buyers. Since this is known in advance the customer may shift their power demand into times with low prices and thereby pay less for per unit of energy consumed. The downside is that the customer may have to purchase energy at peaks in the energy price market and pay more than they would have in a static tariff. Therefore, it is interesting to investigate if these modern ToU tariffs, also known as dynamic tariffs, can help reduce the cost of electricity.

In Figure 8 the hourly day-ahead market price for 2024 is shown in €/MWh. These serve as the base for the electricity price. In addition to the market price, fees and taxes are also included in the final the final electricity price. The price components are as follows [34]:

- Market price: $\varnothing 7,957 ct$/kWh (2024)
- Net usage fee: $11,53 ct$/kWh
- Concession fee: $1,66 ct$/kWh
- Profit margin: $5 ct$/kWh
- Other fees: $1.88 ct$/kWh
- additional costs: $2.15 ct$/kWh
- Electricity tax: $2.05 ct$/kWh
- Value added tax (VAT): 19%

This allows us to calculate the price per kWh depending on the market price p_{kWh} the following way:

$$(p_{\text{kWh}} + 11.53ct + 1.16ct + 5.00ct + 1.88ct + 2.15ct + 2.05ct) \cdot 1.19 = 38.36ct$$

In the past 16 years the price of electricity production has increases by $\approx 2\%$ per year. We will continue this trend in our simulation and increase the production cost of electricity annually by 2%. During the simulation period we assume that the taxes and fees stay the same [13].

5.2. Modeling of feed-in tariffs

In Germany the feed-in price per kWh is guaranteed under the Renewable Energy Act depending on the installation date for the next 20 years. For rooftop mounted photovoltaic systems the price depends on the installed capacity and whether the power produced is fed into the grid completely or only partially. In our model we

want to directly consume the power generated by the photovoltaics. We will only feed-in partially any surplus production we can not consume or store. For new systems installed between 1st of February 2025 and 31st of July 2025 with less than 10kWp installed a price of $7.94ct$/kWh is awarded for partial feed-in. For larger systems between 10 and 40kWp $6.88ct$/kWh is paid [7]. We will use these two values in order to price electricity sold to the grid depending on the installed photovoltaic capacity.

After 20 years of guaranteed feed-in we assume that feed-in tariff is not extended and any unused solar energy is dumped or exported to the grid without compensation.

5.3. Negative electricity prices

In the past years falling prices for photovoltaic systems led to a huge increase in solar power capacity. As a result during good conditions for solar electricity generation more often the spot market prices per kWh drop, sometimes even becoming negative. This is a problem for electricity companies paying fixed feed-in rates to residential PV systems owners as they have to sell these overproduction at a loss. In February 2025 the German government passed a law to pause feed-in guarantees during times of negative electricity spot prices [17].

In 2024 there were 457 hours with negative electricity price over a total of 89 days (on average 5.14 hours for each of these days). The most hours with negative electricity prices occur in spring (March to May) and summer (June to August) accounting for 40% each. In fall (September to November) about 12% of hours with negative prices occur and 18% in winter (December to February). Half of all hours with negative prices occur between 12:00 and 18:00. While the remaining hours mostly happen between midnight and morning [18].

For our modeling we use the spot market prices for 2024 to determine when the feed-in compensation will be paused due to negative prices. During these periods we are still able to feed-in any surplus of energy into the grid but will receive no compensation, i.e. $0ct$/kWh. We want to avoid this as much as possible since it diminishes the revenue generated and negatively impacts economic feasibility.

5.4. Modeling of heating with heat pumps

The move towards more climate neutrality primarily focuses on phasing out fossil fuels. A important factor, in addition to generating electricity, is the heating and cooling in buildings. The most promising residential heating methods are district heating for entire neighborhoods or heat pumps for individual buildings. Since district heating is centrally planned and is not available in many cases, we will focus on heat pump-based heating and model them accordingly.

The heating demand of a flat or house can be estimated using two key parameters: the heated area and the specific heat demand per square meter. The heating demand strongly on the buildings insulation quality. For example a newly built house must be constructed such that the heating demand is at most $40\text{kWh}_{heat}/m^2$. The heat demand for existing buildings typically ranges from $60 - 100\text{kWh}_{heat}/m^2$ whilst old buildings

can have demand of up to 200kWh$_{heat}/m^2$. Table 1 shows the heating demand for typical building sizes and types.

	new building (40kWh$_{heat}/m^2$)	existing house (60kWh$_{heat}/m^2$)	renovated old building (150kWh$_{heat}/m^2$)	old building (200kWh$_{heat}/m^2$)
$70m^2$	2800	3600	10500	14000
$100m^2$	4000	6000	15000	20000
$150m^2$	6000	9000	22500	30000

Table 1: The heat requirement in kWh$_{heat}$ for different house types and sizes.

Simply put, a heat pumps works by transferring heat from a medium (e.g. water, the ground or outside air) with water used inside the house to heat or as domestic warm water. The efficiency of the heat pump varies significantly depending on the heat source between a factor of 3.0 and 5.0. This means 1kWh of electricity produces $3-5$kWh$_{heat}$. For Germany the most common type of heat pump used are air-water systems with an efficiency coefficient of $3.0-4.0$. In Table 2 we use a factors of 3.5 to show how much electricity is required to satisfy the heating demand estimated in Table 1.

	new building	existing house	renovated old build	old building
$70m^2$	800	1059	3000	4000
$100m^2$	1143	1714	4286	5714
$150m^2$	1714	2571	6429	8571

Table 2: Electricity needed in kWh to satisfy the heating demand per year using a air-water heat-pump with an efficiency of 3.5.

In our model, we use the annual electricity consumption of the heat pump (in kWh) as input. This way the actual heat demand and heat pump used is not fixed in the model and making it easily extendable in the future (e.g. by changing type of heating system). The power consumed is used to generate heat for both space heating and domestic hot water. According to Stene [32], this can be split $25-45\%$ for hot water and $55-75\%$ for heating. Going forward we set 40% of the energy is used for hot water assuming a well-insulated buildings. In Germany heating is primarily required during the colder half of the year, from October through the end of March. The electricity used for heating is evenly distributed across these days. The electricity required for hot water, in turn, is evenly distributed throughout all 365 days.

5.5. PV power generation

The European Commission provides irradiance data for the European Union through the Photovoltaic Geographical Information System (PVGIS). By specifying the loca-

tion, slope, and azimuth angle, we can obtain hourly irradiance data for 2024. Utilizing the method specified in section 2.5 the annual power generated by the solar panel placement is calculated.

According to Beck et al. [4], a resolution of 15min for generation and consumption is sufficient to keep errors below 5% when simulating over the time span of a year. To increase the accuracy of our simulation, we linearly interpolate the solar power data to obtain a power generation curve with a 15 minute resolution.

5.6. Modeling of electrical consumption

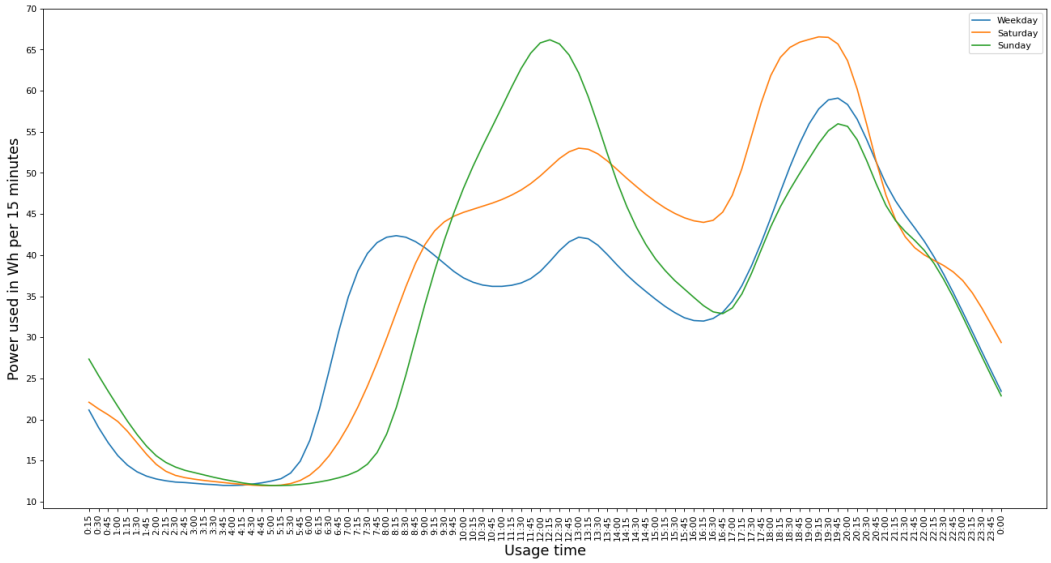

Figure 9: Standard consumption profile for the winter half of the year split into weekdays, Saturdays and Sundays. (Data provided by Bundesverband für Energie- und Wasserwirtschaft e.V.)

In order to accurately estimate how much of the electricity generated by the PV system is directly used and how much can be sold or stored, we need to know how much energy is consumed at point in time. The amount of electricity used strongly depends on the size of the household, i.e., the annual total electricity usage. The "Bundesverband für Energie- und Wasserwirtschaft e.V." (BDEW) provides consumption profiles for various types of consumers (e.g. households, agriculture, or commercial) called Standard Consumption Profiles (SCP). The SCP H0 represents the consumption of household. These profiles aggregate data from a large number of households to provide a reliable estimation of the typical energy consumption profile for each day of the year. The typical consumption pattern for a household is very similar for Monday through Friday (work days) and is therefore further aggregated. For each week the profile consists of a representative work day, Saturday and Sunday. Furthermore, the profiles split the aggregation into winter, summer and the transitional periods between

to accurately account for the changing demands, such as lighting needs. Finally, the profiles are normalized to a electricity consumption of 1000kWh per year [14].

We use this profile to obtain a reasonable estimate of electricity usage over time. The values given in 15 minute intervals are scaled to fit the annual electricity demand of the household to model. Using this method, we obtain a curve that models the household's power consumption.

5.7. Modeling of battery storage

During times when the photovoltaics produce more energy than consumed, any surplus of electricity generated will be tried to store in the battery storage, if possible. We model the PV battery system as DC-coupled, meaning the battery stores the charge coming from the PV directly in DC. Since PV systems also generate DC, no conversion is required to store the energy. Nonetheless charging the battery results in a loss of $5-15\%$. We will model this loss using the average efficiency of 90%. Additionally, any power discharged from the battery must be converted from DC to AC. For this process, an efficiency of 98% is common for modern hybrid inverters. Therefore, additional 2% of the energy is lost during the conversion. Overall, this means that of each kWh of solar energy produced and stored, only 0.882kWh (88.2%) is usable in the household.

Another option for using a battery storage is to charge if from the power grid. During this procedure the electricity has to be converted from AC to DC (98%), stored (90%) and converted back (98%). Therefore for each kWh stored only 0.864kWh may actually be used in the household. Due to this loss storing energy from the grid is only economically sensible when using a ToU tariff and purchasing electricity at low prices as otherwise the loss increases the price per kWh consumed. Charging battery storage from the grid greatly increases complexity of the model with regards to energy flow and we will therefore not investigate it in this thesis.

5.8. Modeling of electrical vehicle

To accurately model a specific electric vehicle, we use four key characteristics: distance driven per year, average power consumption per kilometer, battery size, and a usage/charging profile. The electric vehicles characteristics used in the simulation are specified in Table 3.

The typical German car is driven 13.232km per year. This distance is equally distributed across all usage days, based on the specified average power demand per kilometer. The average electric vehicle has a power demand of 0.189kWh/km and a battery size of 71.44kWh [9].

For simplicity we restrict our modeling to a single car used from Tuesday through Thursday (e.g. to drive to and from work). Consequently, the car may be charged any time not in these usage periods.

A recent development is the use of electric vehicles as additional battery storage. This technology is called Vehicle-to-Home (V2H) or Vehicle-to-Grid (V2G), depending on whether the battery is discharged into the home for private use or into the

Characteristic	Value
Usage	Tuesday-Thursday 8h-18h
Distance per year	13323km
kWh per km	0.189
kWh per year	2518
Battery size	71.44kWh

Table 3: An example of the car usage using average battery size, usage and consumption of electric vehicles.

power grid. The usage times of the vehicles are particularly important when analyzing this technology, as they can only serve as storage when not in use and connected to a wall box at home. V2H-ready vehicles require the battery's state of charge to remain between 30% and 80% to prevent battery degradation and ensure safe charging. Therefore, V2H allows for 50% of the electric vehicles battery to be used as additional storage.

Similar to the stationary storage, the electric vehicle's battery has a charging efficiency of 90% and a 2% energy loss during AC/DC conversion.

5.9. Modeling of system cost

The main goal of using photovoltaics is to either earn money directly by selling the electricity or to reduce one's own cost of electricity in order to save money. For these users it is most important to size the PV and battery storage system in a way that maximizes profit with regard to the expected lifetime of the system (usually 20-25 years). In 2022, "the mean price of PV installations [was] 1392.1€/$kW[p]$ with a large standard deviation of 284.6€/$kW[p]$ " [27]. This includes a variety of different aspects from the solar panels themselves to electrical work, labor cost, and scaffolding. Many components such as scaffolding or inverters are required only once per installation and therefore become cheaper for larger installations. In Table 4 we show how we price the different components.

In addition to the prices listed, there is a profit margin of 15% on materials and 20% on labor. Using this, we can calculate the price of a PV battery system using the Equation 15.

Component	Category	Price	Symbol
Solar panel	Material	60	mat_{panel}
Panel substructure	Material	70€	mat_{sub}
Panel cables	Material	5€	mat_{cable}
Inverter	Material	200€/kWp	mat_{inv}
Battery	Material	500€/kWh	mat_{batt}
Meter cabinet	Material	1100€	mat_{meter}
Wallbox	Material	900€	$mat_{wallbox}$
Work per panel	Work	35€	$work_{panel}$
Meter cabinet	Work	400€	$work_{meter}$
Inverter	Work	400€	$work_{inv}$
Battery	Work	100€	$work_{batt}$
Wallbox	Work	900€	$work_{wallbox}$
Scaffolding	Other	18€/m^2	$c_{scaffolding}$
Fees	Other	350€	c_{fees}

Table 4: Prices for the different components of a photovoltaic and battery storage installation with n being the number of modules.

$$
\begin{aligned}
C_{total} = &((mat_{panel} + mat_{sub} + mat_{cable}) \cdot n + mat_{inv} \cdot pv_{kWp} + mat_{batt} \cdot batt_{kWh} \\
&+ mat_{meter} + mat_{wallbox}) \cdot 1.15 \\
&+ (work_{panel} \cdot n + work_{batt} + work_{meter} + work_{inv} + work_{wallbox}) \cdot 1.2 \\
&+ c_{scaffolding} \cdot l \cdot w \\
&+ c_{fees} \\
= &((60€ + 70€ + 5€) \cdot n + 200€ \cdot pv_{kWp} + 500€ \cdot batt_{kWh} + 1100€ + 900€) \\
&\cdot 1.15 \\
&+ (35€ \cdot n + 400€ + 400€ + 100€ + 900€) \cdot 1.2 \\
&+ 18€ \cdot l \cdot w \\
&+ 350€
\end{aligned} \tag{15}
$$

$$
\begin{aligned}
pv_{kWp} &:= \text{Amount of PV installed in kWp} \\
batt_{kWh} &:= \text{Size of installed battery storage in kWh} \\
l &:= \text{Length of the building in meters} \\
w &:= \text{Width of the building in meters}
\end{aligned}
$$

5.10. Energy system model

The energy system, including all components, is visualized in Figure 10. The power sources are either photovoltaics, the power grid or the electric vehicle (if Vehicle-to-Home technology is available). The consumers include the household modeled via the

Standard Consumption Profile, the heat pump and the electric vehicle. Any surplus of power generated is either stored in the battery, electric vehicle or sold to the power grid. As described in earlier sections each power conversion between AC and DC results in a 2% energy loss. As basis for this model, we used the modeling done by Boeckl and Kienberger [6], which we extended and adapted.

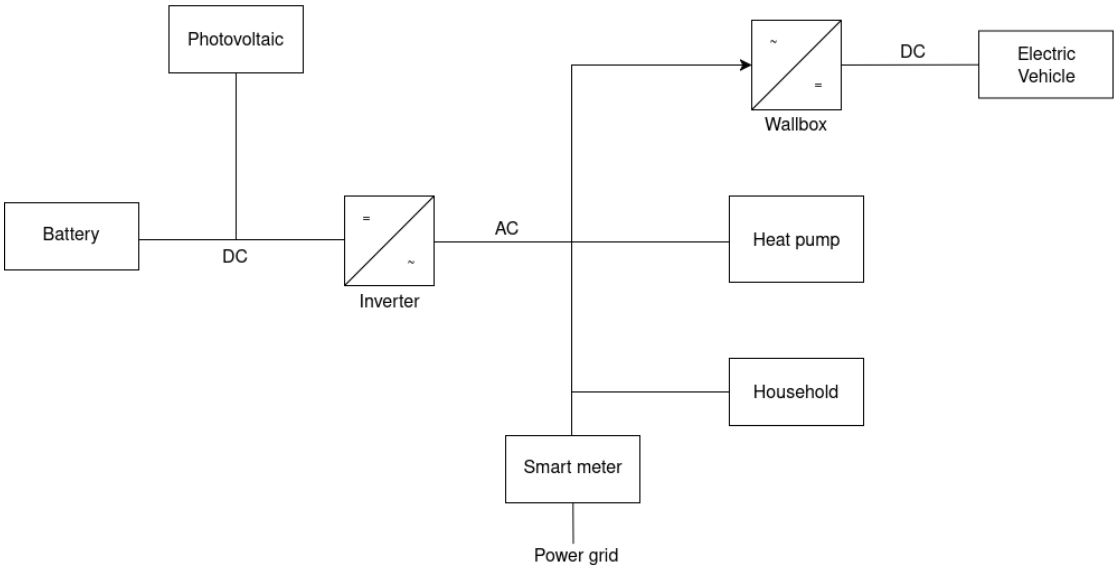

Figure 10: A visualization of the energy system model including all components and power conversions.

6. Simulation of energy systems

The goal of the energy system model is to determine which storage size is optimal in conjunction with the photovoltaic installation. Since load and power generation are unequally distributed throughout the day we evaluate the system using a discrete time simulation over the period of a year. As the sample year we have chosen 2024 due to good availability and recency of the data. The results of the simulation is then projected over an assumed lifetime of 20 years (guaranteed duration of feed-in compensation).

6.1. Simulation step size

The accuracy of a discrete time simulation is dependent on the time resolution chosen. Beck et al. [4] concluded "for optimal sizing of the PV power and the storage capacity a resolution of 60 minutes is found to be sufficient". They further explain that choosing a step size of at most 15 minutes keeps the errors reasonably low. Using these insights we chose our simulation step size as 15 minutes. The household load profiles are already available in a resolution of 15 minutes. The irradiance data used to calculate the yield of the photovoltaics we use linear interpolation to the hourly irradiance data, creating a smoother 15-minute resolution curve. Finally the spot market price data only changes every hour. Therefore the hourly values are spread over four intervals of 15 minutes with the same value.

6.2. Simulation behavior

The target of this simulation is to find the optimal size of storage. In order to do this we will simulate different sizes of storage from $0 - 20$kWh in 1kWh intervals. For each different storage size the simulation is run three times. First to evaluate the base model, second to simulate with feed-in tariff and third without feed-in compensation. The parameters are chosen according to the modeling in Chapter 5. Using the sample year data, we can project the behavior of the simulation to the full simulation length.

At the start of the day the electricity prices, feed-in compensation and difference between electricity generation and consumption are forecast. Using these predictions we plan the electric vehicle charging during times of PV overproduction and/or lowest prices. Additionally we calculate buffers for the storage in order to improve charging behavior (see 6.4). Using these plans the simulation then process through the day using 15 minute steps. For each step the following steps are checked:

1. Obtain power difference between demand and production
2. Charge/Drain battery storage
3. Charge/Drain EV battery
4. Buy/Sell electricity to/from the grid

If the photovoltaic produces more energy than is consumed the surplus is first directed to the battery storage. Any remaining surplus is then redirected to charge the electric vehicle if possible. Finally any electricity unable to be self-consumed or stored is sold according to the feed-in tariff.

If the demand for power is larger than the production - often in the evening, night and morning - the battery storage is drained in order to supply the difference in power. If the battery storage cannot meet the demand and the electric vehicle is capable of bidirectional charging, the power is drained from the battery of the electric vehicle. Lastly, if the demand for electricity can not be satisfied by PV or stored energy, it is purchased from the electricity grid for the price at this point in time specified by the chosen electricity tariff.

6.3. Simulation baseline

The baseline model is the benchmark the model is evaluated against. In 6.3 we modeled the baseline as using a static electricity tariff, no photovoltaics, no battery storage, a heat-pump and the same electric vehicle. In general this baseline can be adjusted to be any valid model for the simulation.

In our case the baseline model represents the model using only the grid to supply its electricity demand. Since no PV or storage have to be installed the only cost incurred by the baseline model is the cost of electricity.

6.4. Battery storage strategies

We expect that a regulation passed in Germany in February 2025 pausing any feed-in compensation pausing during times of negative electricity prices will have an effect on how to operate a battery storage. In detail this means that during periods of negative market prices - often occurring during peak production conditions for PV - the feed-in is set to $0ct/\text{kWh}$, increasing the importance of storing energy during these windows. In order to investigate this we define two strategies: *Naive* and *Lookahead*.

The *Naive* strategy simply charges the battery storage if a surplus of electricity is generated by PV. We suspect that this will result in a high state-of-charge (SOC) earlier in the day and potentially cause over-production of photovoltaics to be fed into the grid during hours of negative prices and therefore sold without compensation. The storage is discharged if there is higher demand for energy than is produced by PV.

The *Lookahead* strategy tries to minimize the amount of electricity fed into the power grid during times of negative spot market electricity prices. In order to do so a buffer is reserved in the battery storage for each time step for each day. This buffer is set to the total amount of PV overproduction occurring during negative electricity prices at later time steps during the same day. For time steps with underproduction the buffer is reduced by this amount since it frees up capacity in the storage.

The charging now distinguishes two cases: Charging during negative and non-negative prices. Charging during non-negative prices sets a new virtual maximum capacity for the storage being the storage capacity minus the reserved buffer. The

storage is then at most charged up to this virtual limit. During negative prices the storage is charged disregarding the buffer as normal. Discharging the storage occurs as usual in both cases.

This strategy does not change the total amount of electricity charged or discharged. It only shifts the charging periods to prioritize times without compensation. This may increase the revenue from electricity sold to the grid.

6.5. Electric vehicle behavior

According to the usage profile a minimum charge is calculated for each day such that the electric vehicle may always be used without the risk of running out of charge. This lowest charge threshold is the amount of electricity needed between two consecutive charging day (e.g. Monday and Friday).

Charging is done in two phases: Primary charging is done via "slow"-charging. This means the EV battery is charged using the surplus electricity generated by PV over the course of the day. Secondary charging is done using "fast"-charging during the period with lowest electricity cost at maximal charge-rate. These two phases may overlap e.g. during noon when electricity is cheap due to high PV production on the home and in the grid.

If the EV is capable of V2H the battery of the electric vehicle is discharged during periods of insufficient PV generation. The battery is drained only until either the minimum charge limit or the lower V2H threshold of 30% is reached.

6.6. Economic evaluation

In order to be able to compare the economics of different models we define to total yearly system cost c_{total} as the sum of the system amortization rate $c_{amortization}$ and the annual electricity cost $c_{electricity}$ minus the compensation awarded for selling electricity to the grid $c_{feed-in}$.

$$c_{total} := c_{amoritization} + c_{electricity} - c_{feed-in} \tag{16}$$

The annual amortization rate is the fraction of the total system cost - as modeled in Section 5.9 - over the lifetime of the simulation T_{sim} in years.

$$c_{amortization} := c_{system}/T_{sim} \tag{17}$$

Since we model static as well as dynamic tariffs the price of a unit of electricity is a function dependent on time $p_{buy} : T \to \mathbb{R}$ defined over the simulation time steps T. The amount of electricity purchased is given by the function $a_{buy} : T \to \mathbb{R}$. The total price for electricity is the sum of the amount of electricity bought at each time step multiplied by the current price.

$$c_{electricity} := \sum_{t \in T} p_{buy}(t) \cdot a_{buy}(t) \tag{18}$$

Analogously we can define the compensation for fed-in electricity. $a_{sell} : T \to \mathbb{R}$ being the amount sold per time step and $p_{sell} : T \to \mathbb{R}$ being the price it was sold for.

$$c_{feed-in} := \sum_{t \in T} p_{sell}(t) \cdot a_{sell}(t) \tag{19}$$

The total profit of the system over the duration of the simulation then is the difference of the yearly total cost and the yearly baseline cost c_{base} over the number of years in the simulation T_{sim}.

$$profit := (c_{total} - c_{base}) \cdot T_{sim} \tag{20}$$

7. Simulation results

We define the following key figures relevant for the investigation and evaluation of the different PV and battery storage systems:

Economic Profit: The economical profit is the difference in annual cost of the baseline model and the electricity costs and amortization rate of the PV and battery storage system.

Self-consumption rate (SCR): The self-consumption rate defines the amount of electricity produced by the photovoltaic system actually consumed by the household itself.

Autarky: The fraction of electricity demand satisfied by power from the photovoltaic installation.

For the individual household a high degree of autarky is desirable since it directly reduces the amount of electricity that must to be purchased from the grid. Since the cost of self-produced electricity is low compared to electricity tariff prices this directly reduces the cost of power overall. Additionally, many (potential) users interested in photovoltaics want to increase their independence from the electricity grid [25].

Grid-connected photovoltaic systems with low SCR can have a negative impact on the grid, contributing to high volatility and load within the distribution infrastructure. Increasing SCR helps to reduce the amount of electricity transported from the modeled household. This can help to reduce the negative impact of PV power. When combined with a high degree of autarky it results in even less energy that must be transported over the distribution infrastructure further reducing cost and helping to stabilize the grid [24].

7.1. Case study parameters

Property	Case Study 1	Case Study 2
Size	$19.2m \times 10.8m$	$15m \times 9.2m$
Annual electricity usage	4000kWh	3000kWh
Heating (electricity)	3300kWh	2500kWh
Panel count	72	44
PV peak power	32.4kWp	19.8kWp
Feed-in compensation	$6.88ct$/kWh	$6.88ct$/kWh

Table 5: Parameters for the modeling of the two case study objects. The heating demand is given as the kWh used by a air-water heat pump according to the modeling in 5.4. The PV placement represents a full usage of all roof surfaces (including north-facing) using the *Vertical* algorithm.

We use the case study object defined in Section 4.1 and extend it with the necessary parameters to optimally size the storage. Both case studies use an air-water heat pump and an electric vehicle. The PV system installed is calculated using the *Vertical* placement algorithm due to its effective translation into practical applications. We utilize the entire roof - including north-facing surfaces - to place PV panels. Due to low cost and improved electricity generation of modern PV panels, even using only low irradiance levels, the installation of panels on the north side of the house has become economically feasible in recent years. The annual electricity usage is modeled to represent a four-person household in Case Study 1, and a three-person house hold in Case Study 2. The amount of electricity used for heating is calculated using the method in Section 5.4.

7.2. Evaluation of baseline simulation

The baseline model as described in Section 6.3 represents the base version for each object without a photovoltaic and storage system. Therefore, the cost of the baseline is the annual cost for purchasing electricity to satisfy the power demand using a traditional static electricity tariff. For Case Study 1 this results in a cost of $3,993.60$€ per year for 9818kWh. Case Study 2 purchases $8,018$kWh per year for the price of $3,331.60$€. Since no PV is utilized in the baseline model autarky and self-consumption rate are both 0% for both case studies.

7.3. Optimal storage sizes

In order to answer the question how to determine the optimal storage size we will evaluate each of the key variables defined in Section 7. The first and most important key figure we evaluate is economic profit since it will most significantly determines the feasibility of the installation.

Economic profit

In Figure 11 we can see how the total electricity cost, system cost and total cost develop for storage capacities from $0-20$kWh. As *electricity cost* we describe the residual cost of the electricity purchased minus the revenue generated by selling photovoltaic power to the grid. We can observe this for both case studies even without battery storage the system is profitable through just using PV on its own. Case study 1 generates an annual profit of 907€ and Case Study 2 a profit of 596€ per year.

Furthermore we observe that the profit at first increases with additional storage capacity the profit increases due to a steep decline in electricity cost. This profit growth achieves a maximum of 1214€ per year at 8kWh storage capacity for Case Study 1 and 822€ at 6kWh for Case Study 2 respectively. As Figure 11 shows this is due to a diminishing decrease in electricity cost with additional capacity, which is insufficient to cover the linear growing cost for additional battery storage.

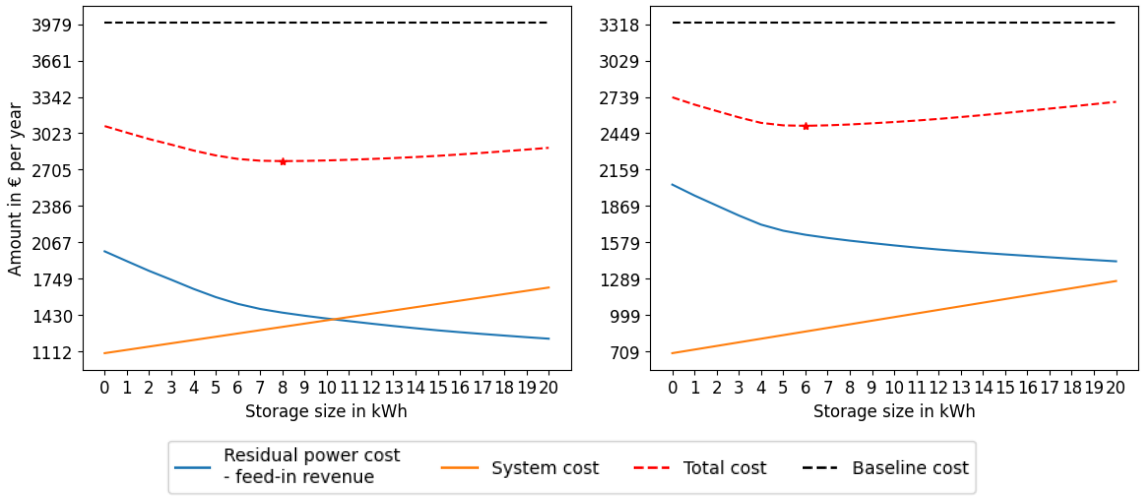

Figure 11: A comparison of yearly total cost consisting of electricity cost and year system amortization rate against the cost of the baseline model over the lifetime of 20 years for Case Study 1 (left) and Case Study 2 (right). The star represents the storage size with minimal total cost/maximal profit.

The optimal capacity for Case Study 1 can be explained by the larger PV installation, generating more power allowing to more efficiently utilize the additional storage capacity even during sub-optimal conditions i.e., during spring, fall, or cloudy weather. Furthermore the larger demand for electricity allows for more self-consumption during overall and therefore a large decrease to electricity cost.

Self-consumption rate and autarky

This section explores in more detail how battery storage size influences the SCR and autarky (see Figure 12). For both case studies using no battery storage results in a self-consumption rate of 24.2% and 27.8%, respectively. With additional battery storage capacity the SCR monotonously increases and therefore achieves its maximum (within the investigated storage size range) at 20kWh battery storage with 42.3% and 52%, respectively. The SCR at first increases rapidly in linear growth before flattening out and following a logarithmic growth with diminishing return. The rate of increase towards the previous step slows down quite fast and drops below 3% at 6 and 7kWh and to below 1% for 13 and 14kWh. This means that for further increases large investments into additional storage capacity are necessary.

The autarky behaves similar to the self-consumption rate starting at 38.7% and 32.2%, monotonously growing to its maximum 61.7% and 54.6% at 20kWh storage capacity. The first break-point for increase in autarky is 6kWh for Case Study 1 and 7kWh for Case Study 2. The rate of change only drops below 1% at 15kWh and 16kWh, respectively. This means its growth slows down less than the SCR but still requires a large amount of additional storage capacity for small improvements, especially beyond the second break-point.

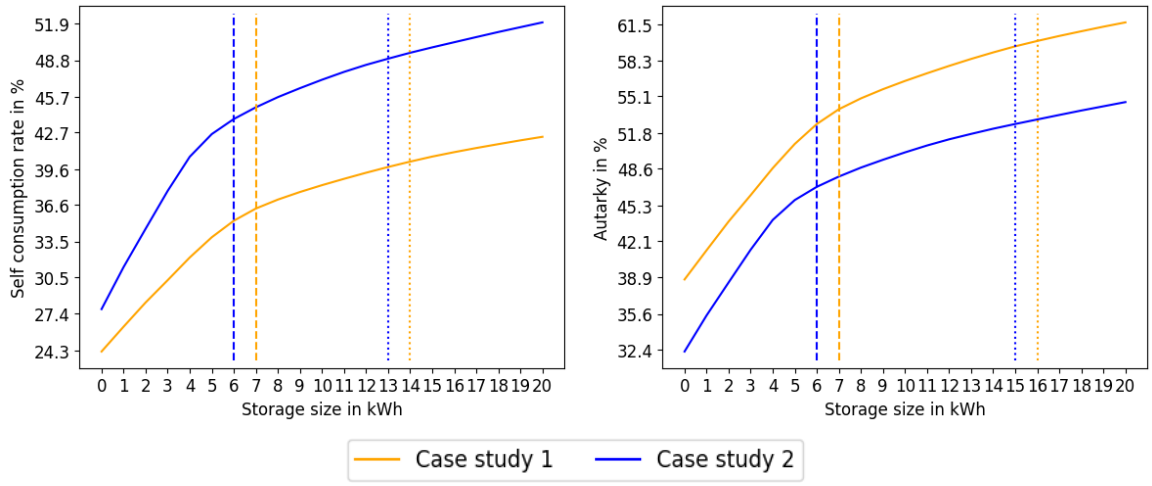

Figure 12: The right graph shows the development of autarky with increasing storage size for Case Study 1 and 2. The left graph shows the increase in self-consumption rate for both case studies. The dashed and dotted lines indicate when the change threshold falls below 3% and 1% respectively.

Lastly we can observe that the self-consumption rate and autarky are inversely correlated with regard to the size of the installed PV capacity. Case study 1 has a significantly larger PV installation when compared to Case Study 2 and their relative electricity demand. This expresses itself in the lower SCR when compared to Case Study 2. At most 40% of the electricity generated is consumed directly whilst 60% is fed into the power grid. Case study 2 in turn is able to consume up to half of its produced power. The autarky displays the reverse behavior. The larger relative PV installation of Case Study 1 allows to satisfy more of it's electricity demand up to a yearly autarky of nearly 62%.

Discussion

Using the insights generated we can now discuss how to optimally size the storage. For this we will view two distinct customer groups for PV battery storage systems. The first group aims to maximize only economic profit. For this group the optimal storage size is 8kWh for Case Study 1 and 6kWh for case study 2 due to maximal profit over the baseline model.

The second group of customers, while also interested in profitability, at the same time try to increase their environmental friendliness and sustainability. Therefore they want to achieve a high degree of autarky and high self-consumption rate. For these goals the optimum is not as clear as for the first group due to the strictly monotonous increase with storage capacity. Since the PV battery storage system is profitable for all evaluated storage sizes we observe a trade-off between increasing autarky as well as SCR and lowering the profit margin. The first break-point lies before the economic optimum and choosing it would therefore result in optimizing neither profit nor SCR/autarky.

We would recommend to choose a value between the economic optimum and the second break-points of autarky and SCR. While going beyond the second set of break-points does increase both autarky and SCR, the gain is very small ($< 1\%$) and users would have to decide if it is worth the additional financial investment and resources.

7.4. Impact of storage charging strategies

In this section, we analyze the impact of using the *Lookahead* charging strategy compared to greedily charging any surplus PV production into the storage using the *Naive* strategy. In Figure 13 we investigate an example day with negative electricity prices during 10:15 in the morning and 16:00 in the afternoon. As we can see the *Naive* strategy charges the storage as soon as the PV produces more energy than is used. The storage reaches full charge at 10:15. Therefore any overproduction of energy would either be sold to the grid without compensation or has to be stored in an additional storage, e.g., the electric vehicle. The *Lookahead* strategy reserves a buffer to minimize

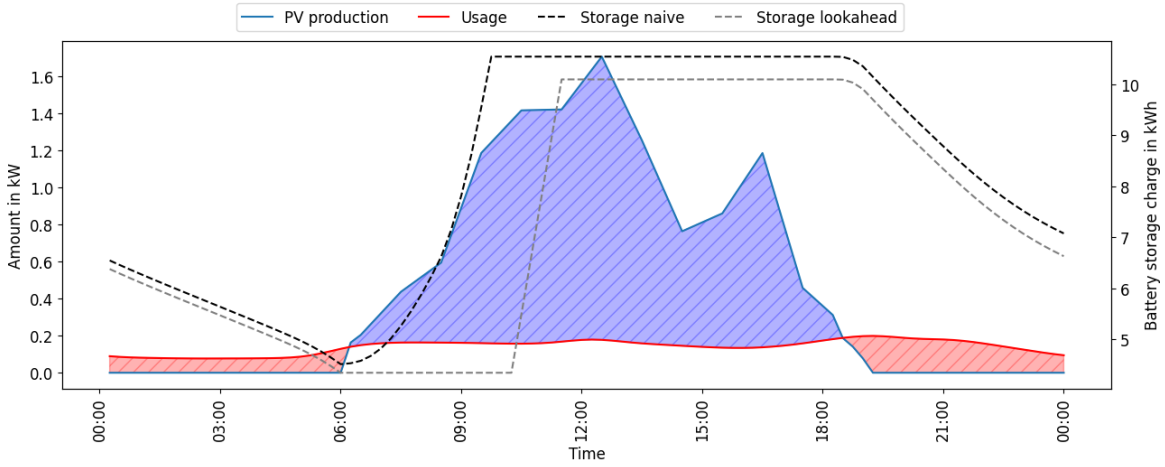

Figure 13: A comparison of battery storage state in Case Study 2 over the course of a day (12th of May) with negative electricity prices during 9:15−16:00. The *Naive* charging reaches full-storage capacity at 10:15 hours. The *Lookahead* method shifts the charge towards later hours of the day such that the battery storage is fully charged at 12:00. The storage used has a maximal capacity of 10kWh.

the amount of electricity that is fed into the grid without compensation. This causes the storage not to be charged until 10:15 when the period of negative prices starts. The electricity is then stored until the battery is full at 12:00. Due to the limited size of the storage and high production of PV, the total surplus cannot be stored. However an additional two hours of feed-in compensation is achieved this way.

Over the course of a whole year these small savings compound to increase the revenue generated by selling electricity to the grid. In Figure 14 we can clearly see that for both case studies the *Lookahead* strategy is able to increase profit. The annual profit of Case

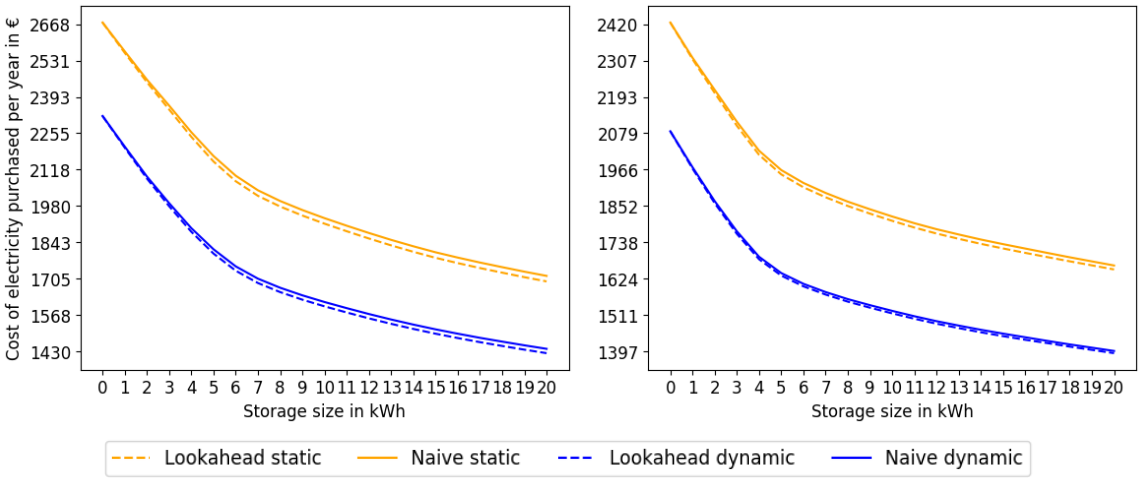

Figure 14: A comparison of yearly profit between different tariff types and storage strategies between Case Study 1 (left) and Case Study 2 (right).

Study 1 increases by up to 40€ (3.3%) per year and Case Study 2 by up to 27.5€ (3.3%) per year. The *Lookahead* strategy relies on prior knowledge of the negative electricity prices and exact photovoltaic power generation. In reality the photovoltaic power would have to be estimated introducing error. The values calculated therefore only represent a theoretical upper bound on the achievable financial improvement by employing the *Lookahead* strategy. However these results are a good indicator that using a smart battery storage management system profit can be increased.

7.5. Comparison of electricity tariffs

Recent developments in electricity tariffs include Time-of-Use tariffs that enable the customer to buy the power at (day-ahead) market prices. Consequently, while the user is able to profit off price dips, they also take on the risk of needing to pay high prices during peaks. We investigate if these dynamic tariffs allow the user to reduce their energy cost when used in combination with PV and battery storage. Figure 15 shows how the average electricity price (aggregated over the year) behaves per hour. We can clearly see two peaks in the morning and evening when consumption is typically high (see Figure 9) and dips after midnight and during noon. In the early morning hours electricity demand is low, causing low prices whilst the dip at noon is caused by peak PV production.

When examining the cost of electricity between dynamic and static tariffs in Figure 16, we can clearly observe a significant decrease in cost by $275.90 - 353.50$€ $(13.2 - 18.4\%)$ for Case Study 1 and $267.20 - 340$€ $(14 - 16\%)$ for Case Study 2. The difference between the average dynamic price of $35.165ct$/kWh and the static price of $39.50ct$/kWh is only 11%. This means that switching to a dynamic tariff increases profit further than just having a cheaper mean price. The additional $2.2 - 7.4\%$ increase is the result of effectively using stored photovoltaic power during the evening

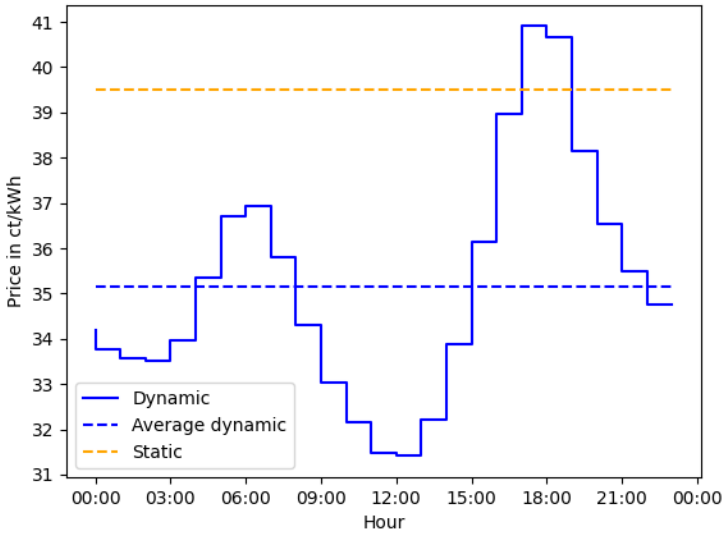

Figure 15: A comparison of dynamic electricity price, average dynamic electricity price and static tariff per hour aggregated over the whole year.

peak as shown in Figure 13.

The decrease below the average dynamic price can also be seen in Figure 17. Without any storage the price per kWh lies above the mean dynamic electricity price with $37.57ct$/kWh for Case Study 1 and $37.27ct$/kWh for Case Study 2. With increasing storage capacity however the price quickly drops below the average dynamic price, then slowly rises by a small amount. At the same time the amount of electricity bought decreases monotonically with increasing storage size causing overall electricity cost to drop with increasing storage capacity. For storage capacity of 5 kWh and above this results in a reduction of electricity unit cost of at least 1.7% and up to 2.6% or $0.65 - 0.85ct$/kWh cost reduction. This further proves that dynamic tariffs and use of battery storage are capable of reducing electricity cost further than just the gap by making use of electricity price peaks and dips. This improvement was achieved by simply using the storage as a buffer instead of optimizing for maximal profit. Using a smart battery storage system, discharging times could be optimized to further reduce electricity costs.

7.6. Impact of V2H usage

Bidirectional charging for electric vehicles is a promising technology that easily provides power storage to homes if a V2H-capable electric vehicle is owned by simply connecting it to the wallbox. According to our modeling the EV is used as secondary storage. This means it is only charged when the battery storage is full and discharged if the battery storage is empty.

When storing electricity in the electric vehicle and using it at a later time only

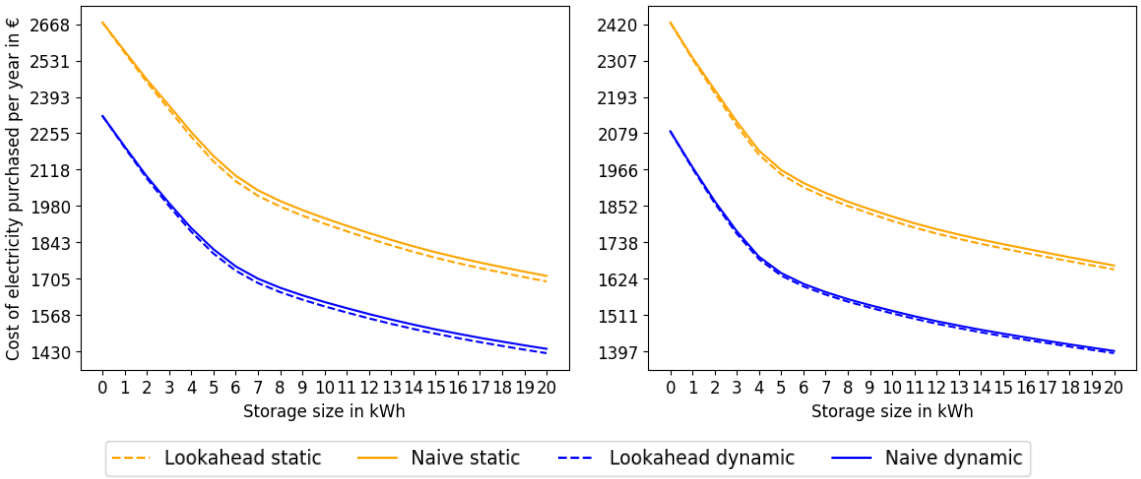

Figure 16: A comparison of yearly electricity cost between different tariff types and storage strategies between Case Study 1 (left) and Case Study 2 (right).

86.44% (due to two conversion losses plus charging loss) of the power used to charge is available later due to charging and conversion losses. This means that in order for it to make sense to use bidirectional charging over drawing power from the grid a price difference of at least 13.46% must be achieved. For solar power, this is easily achieved due to the large gap between feed-in compensation and electricity prices from the grid. For power from the grid this is only achievable using a dynamic tariff and making use of peaks and dips in electricity prices.

Figure 18 illustrates the average cost of electricity and amount of electricity purchased with and without V2H. It clearly shows a decrease in average electricity cost of $1.1 - 2.2ct$/kWh for both case studies when compared to using an EV without bidirectional charging. The largest improvement is achieved for small storage sizes of at most 4kWh. This is due to a surplus in power generated by photovoltaics in combination with an insufficiently large battery storage allowing for large amounts of solar energy to be stored in the EV. With larger storage sizes this decreases to $1.3ct$/kWh (3.5%) for Case Study 1 and $1.2ct$/kWh (3.3%) for Case Study 2.

On the flip side Figure 18 shows that our modeling of bidirectional charging causes the electric vehicle to draw more power from the grid than it does without V2H. Figure 19 shows that for small storage sizes the decrease in electricity cost as a whole makes the usage of V2H profitable for both case studies. For larger storage sizes the additional power drawn from the grid negates the profits made by lower average electricity cost causing V2H to only generate minor profits or even small losses.

Since V2H is used as a secondary storage the only significant improvement in self-consumption rate is for low storage capacities of less than 5kWh. For larger storage sizes the improvement is less than 1% for both case studies. On the other hand autarky decreases if V2H is used due to additional electricity needing to be purchased to compensate for charge which can not be supplied by a surplus in photovoltaic power. For both case studies autarky decreases by $1 - 2\%$ for storage capacities over 5kWh.

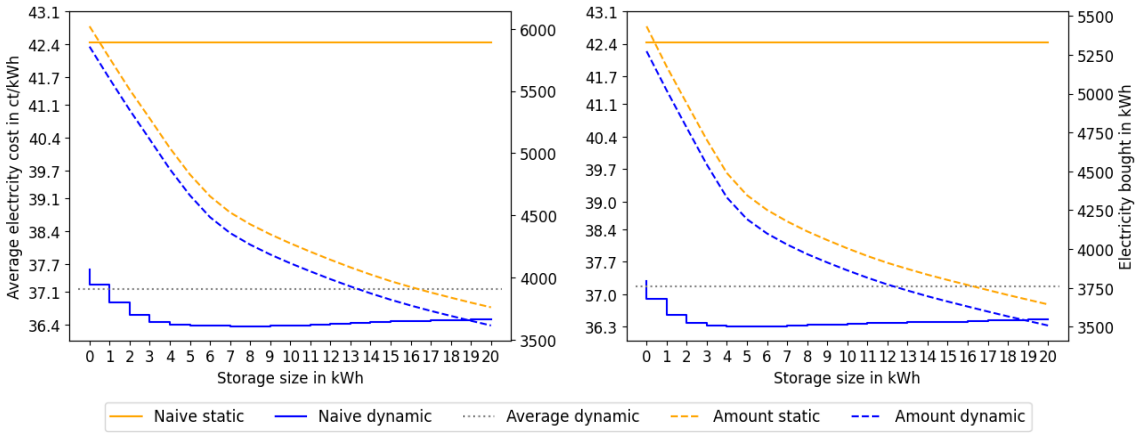

Figure 17: A comparison of average electricity price and amount of electricity bought per year between different tariffs with increasing storage capacity for Case Study 1 (left) and Case Study 2 (right).

Discussion and Limitations

The impact of V2H is highly dependent on the availability of the EV during times of high photovoltaic productivity. We evaluated the performance of a 3 day usage and 4 day charging availability during these windows. Depending on changing the usage profile the performance of V2H usage could vary significantly in both positive and negative directions. It could therefore be interesting to take a more detailed look at V2H usage. Additionally we discharge power greedily when it is required. A more sophisticated algorithm could improve the performance by taking into account differences between charging and discharging periods.

In summary for households with no battery storage or battery storage with a capacity of less than 5kWh our results suggest that V2H is able to improve the usage of surplus photovoltaic power and reduce yearly electricity cost. For larger storage sizes the usage of V2H does not significantly impact the electricity costs or SCR, and negatively impacts the degree of autarky.

7.7. Impact of a 30-Year Lifetime

Modern mono-crystalline solar panels have a long lifetime of up to 50 years and manufacturer-given warranties of $25-30$ years. Additionally, it is interesting to investigate what impact the end of feed-in compensation after 20 years will have on battery storage sizing. To answer this question the simulation is evaluated for the lifetime of 30 years.

The most significant impact is the large drop in yearly amortization costs by one third. This directly causes the total yearly cost for the PV and battery storage system to be reduced as can be seen by comparing Figure 11 and Figure 20. As a result, two things follow: First the optimal storage size for both case studies increases. From 8kWh to 15kWh with a yearly profit of 1605€ for Case Study 1 and from 6kWh to

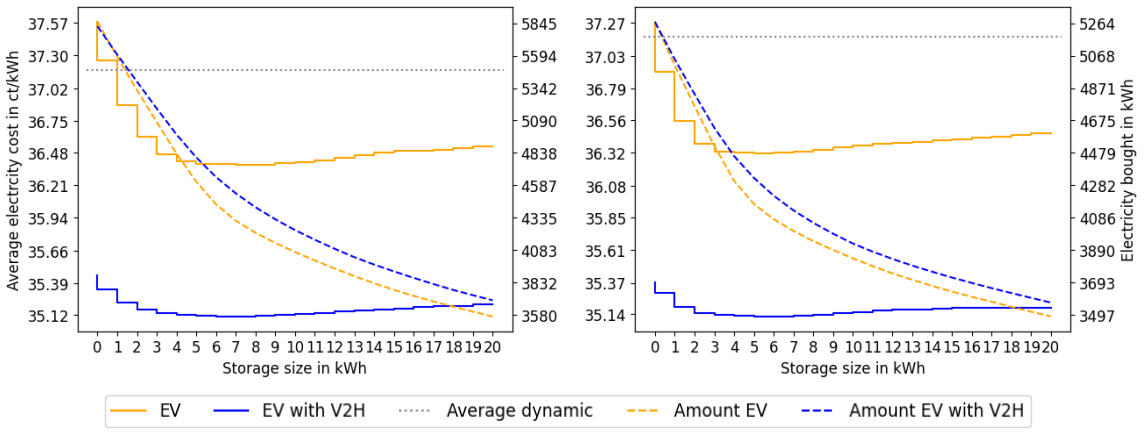

Figure 18: The development of electricity prices using a electric vehicle with and without bidirectional charging and different storage sizes for Case Study 1 (left) and Case Study 2 (right).

11kWh with 1100€ for Case Study 2. This nearly doubles the optimal storage size compared to the 20-year simulation, which is explained by the dropping price and the increased need for self-consumption in the last 10 years. Without feed-in compensation, any power not self-consumed is "wasted" from the operator's point of view.

Additionally, the yearly profit between the optimum and maximal storage capacity of 20kWh is quite low with a difference of 10€ and 50€ annually for both case studies. This makes purchasing additional storage capacity beyond the optimal economic size attractive to increase SCR and autarky. However, the growth of SCR and autarky with increasing storage size however does not change with additional time. This means the growth of SCR drops below 1% after 13/14kWh and the increase in autarky at 15/16kWh, making additional increases less effective.

The *Lookahead* strategy shifts storage charging times to periods without feed-in compensation. Since the feed-in compensation ends after 20 years in our model, the *Lookahead* strategy does only generate profit during the first 20 years. Other strategies may be required to better utilize the storage.

In line with the 20-year simulation, a dynamic tariff reduces the average cost of purchased electricity. Using the larger economically optimal storage sizes the amount of electricity needed to be purchased is further reduced.

The impact of bidirectional charging does not change in comparison with the 20-year simulation.It remains mainly useful for systems with low battery storage size of at most 5kWh.

7.8. Discussion

Using a time-discrete simulation 15-minute resolution we simulated two case study systems and evaluated them according to economic profit, SCR and autarky. Additionally, we investigated the impact of storage management strategies, dynamic tariffs, bidirec-

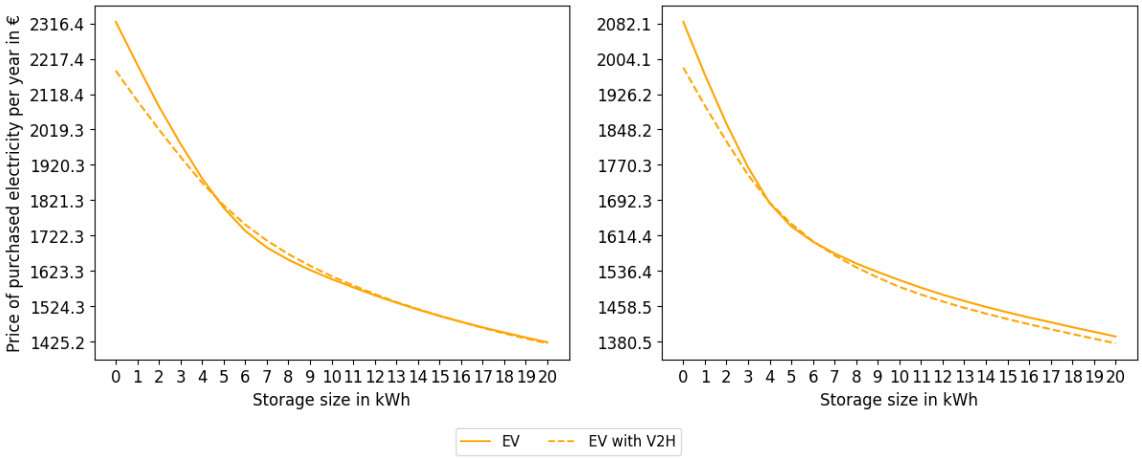

Figure 19: Impact of bidirectional electric vehicle charging and storage size on electricity cost for Case Study 1 (left) and Case Study 2 (right).

tional charging and different lifetimes – with the aim to optimally size the battery storage.

For a lifetime of 20 years the optimal storage size regarding economic profit is much lower then the sizes that maximize SCR and autarky. Both of these factors grow monotonously with storage size but experience diminishing return of less than 1% above 16kWh. Therefore a trade-off between sustainability and profit must be taken into consideration. By increasing the lifetime to 30 years, a 10-year period without feed-in compensation causes the economic optimal storage capacity to nearly double. Due to the PV installation being fixed in size, the storage capacity needs to be large in order to effectively utilize electricity generated during all 30 years. As a consequence, more PV energy can be stored and used causing a higher self-consumption rate and reducing the amount of electricity purchased from the gird resulting in a higher autarky.

The profit generated by using a battery storage can be increased by using smart management strategies. The *Lookahead* strategy was designed to counteract regulation passed February 2025 in Germany pausing feed-in compensation during times of negative sport market electricity prices. By using predictions of power generation and demand as well as spot market price data the charging windows are scheduled such that they overlap with periods without feed-in compensation. Using this strategy profits can increase profit and advocates for the importance of (smart) energy management systems in combination when using an energy storage.

We have shown that bidirectional charging decreases the average cost of electricity when combined with a dynamic tariff. However the total amount of electricity bought is increased by additional charging performed. Therefore only little or no increase in profit is achieved. However, for systems with no battery storage or only small storage capacities of up to 5kWh V2H is able to noticeable reduce cost.

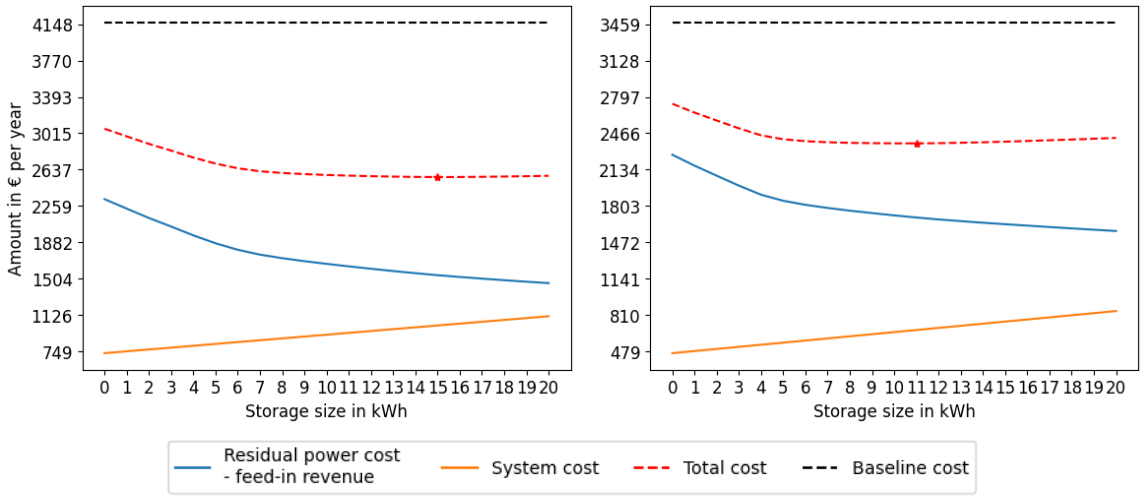

Figure 20: A comparison of yearly total cost consisting of electricity cost and year system amortization rate against the cost of the baseline model over the lifetime of 30 years for Case Study 1 (left) and Case Study 2 (right). The star represents the storage size with minimal total cost/maximal profit.

8. Conclusion

This thesis explored the optimization of rooftop solar panel placement and optimal battery storage sizing. We developed a discrete rooftop model and compared different placement algorithms regarding their maximum power generated, number of panels installed and layout aesthetics, taking into account practical and regulatory restrictions such as obstacles and buffer zones. A time-discrete simulation of an energy system based upon a solar panel placement allows us to optimally size the battery storage capacity for economical profit and sustainability.

8.1. Contribution

Discrete roof model: Modeling the rooftop using discrete cells with precise labeling allows for exact identification of valid solar panel placements. It provides a base for efficiently implementing panel placement algorithms.

Optimal placement: The solar panel placement problem is formulated as an integer program using the discrete roof model as a base. Using a commercial solver the solar panel placement can be solved optimally maximizing the energy generated by the placed solar panels.

Heuristic algorithms: Heuristic algorithms allow for efficient placement of solar panels on the model. Additional constraints including panel orientation, alignment, or symmetry further refine the panel layout in more detail according to practical or aesthetic needs.

Optimal storage sizing: A time-discrete simulation evaluates how the system using PV, battery storage, a heat pump, and electric vehicle behaves over the lifetime of 20 to 30 years. An optimal storage capacity depending on economic profit and sustainability is recommended based on the results.

Dynamic feed-in and tariffs: The inclusion of cutting-edge trends such as dynamic feed-in compensation, spot market electricity tariffs or bidirectional electric vehicle charging are key factors in deciding how to size the system for the future. Their impact on the economic aspect and optimal storage size is evaluated using time-discrete simulation.

8.2. Limitations of work

Requirement of precise labeling: The accurate placement of solar panels requires precise labeling of roof components such as rakes, eaves or obstacles. This process is time consuming and has to take into account regulations which may differ between each federal state.

Usage of aggregated data: In order to estimate electricity consumption the standard load profile for households is used. This model is created by taking the mean of thousands of households representing the average consumption during each time slot of the day. The usage of aggregated data introduces error into this model. Furthermore if the standard consumption profile does not apply to the actual usage of the energy system, e.g., for people working predominantly night shift, the results may differ significantly from reality.

Reliability of solar irradiance data: The power generated by the photovoltaics was estimated using the irradiance data from 2024 for the whole duration of the simulation. Climate change causes the weather to become less predictable and more unstable. Due to this the behavior of the system in reality might be significantly vary from the simulation and from year to year [30].

8.3. Further research

Automatic extraction of roof features: Utilizing machine learning to extract rooftop obstacles aerial or satellite imagery has proven promising for identifying obstacles on rooftops. Extending this to identify more roof features including eaves, rakes and ridges would allow to enhance rooftop models.

Smart battery storage management: In this thesis the battery storage is mostly operated using a greedy approach. The results of implementing a simple storage operating strategy suggest that using a more advanced storage management system optimizing charging and discharging times can have positive a impact on the system.

In depth analysis of V2H: The impact of bidirectional charging on the energy system was only investigated on a surface level during this thesis. A more detailed investigation into different V2H usage profiles and vehicles could lead to more explicit result on when the usage of bidirectional charging is advantageous.

Increased study size: This study only investigates two objects. In order to increase the weight of the results a more sophisticated study with a sufficiently large size has to be done. This provides the opportunity to more accurately pinpoint important influences for optimally sizing PV and battery storage systems.

8.4. Final remarks

This thesis demonstrates a method to solve the solar panel placement problem for residential rooftops with inclusion of regulatory and practical restrictions. Furthermore, it highlights the importance of viewing the rooftop photovoltaic and battery storage as a joint system. Depending on the individual parameters and chosen photovoltaic installation the demand for storage changes significantly. By including cutting-edge developments their impact on economic feasibility and storage capacity make it apparent that there is no universal sizing method but rather has to be chosen according to the demands of the system operator.

References

[1] Irène Apra, Carolin Bachert, Camilo Cáceres Tocora, ÖZGE Tufan, Ondrej Veselỳ, and E Verbree. Inferring roof semantics for more accurate solar potential assessment. *The International Archives of the Photogrammetry, Remote Sensing and Spatial Information Sciences*, 46:33–37, 2021.

[2] Mohammad Aslani and Stefan Seipel. Automatic identification of utilizable rooftop areas in digital surface models for photovoltaics potential assessment. *Applied Energy*, 306:118033, 2022. ISSN 0306-2619. doi: https://doi.org/10.1016/j.apenergy.2021.118033. URL `https://www.sciencedirect.com/science/article/pii/S0306261921013283`.

[3] Mohammad Aslani and Stefan Seipel. Rooftop segmentation and optimization of photovoltaic panel layouts in digital surface models. *Computers, Environment and Urban Systems*, 105:102026, 2023. ISSN 0198-9715. doi: https://doi.org/10.1016/j.compenvurbsys.2023.102026. URL `https://www.sciencedirect.com/science/article/pii/S0198971523000893`.

[4] T. Beck, H. Kondziella, G. Huard, and T. Bruckner. Assessing the influence of the temporal resolution of electrical load and pv generation profiles on self-consumption and sizing of pv-battery systems. *Applied Energy*, 173: 331–342, 2016. ISSN 0306-2619. doi: https://doi.org/10.1016/j.apenergy.2016.04.050. URL `https://www.sciencedirect.com/science/article/pii/S0306261916305104`.

[5] BloombergNEF. Lithium-ion battery pack prices hit record low of 139 usd/kwh, 2023. URL `https://about.bnef.com/blog/lithium-ion-battery-pack-prices-hit-record-low-of-139-kwh/`.

[6] Benjamin Boeckl and Thomas Kienberger. "sizing of pv storage systems for different household types". *Journal of Energy Storage*, 24:100763, 2019. ISSN 2352-152X. doi: https://doi.org/10.1016/j.est.2019.100763. URL `https://www.sciencedirect.com/science/article/pii/S2352152X18305978`.

[7] Bundesnetzagentur. Eeg-förderung und -fördersätze, 2025. URL `https://www.bundesnetzagentur.de/DE/Fachthemen/ElektrizitaetundGas/ErneuerbareEnergien/EEG_Foerderung/start.html`.

[8] Katalin Bódis, Ioannis Kougias, Arnulf Jäger-Waldau, Nigel Taylor, and Sándor Szabó. A high-resolution geospatial assessment of the rooftop solar photovoltaic potential in the european union. *Renewable and Sustainable Energy Reviews*, 114:109309, 2019. ISSN 1364-0321. doi: https://doi.org/10.1016/j.rser.2019.109309. URL `https://www.sciencedirect.com/science/article/pii/S1364032119305179`.

[9] Electric Vehicle Database. Energy consumption of full electric vehicles, 2025. URL https://ev-database.org/cheatsheet/energy-consumption-electric-car.

[10] Tim N.C. de Vries, Joris Bronkhorst, Martijn Vermeer, Jaap C.B. Donker, Sven A. Briels, Hesan Ziar, Miro Zeman, and Olindo Isabella. A quick-scan method to assess photovoltaic rooftop potential based on aerial imagery and lidar. *Solar Energy*, 209:96–107, 2020. ISSN 0038-092X. doi: https://doi.org/10.1016/j.solener.2020.07.035. URL https://www.sciencedirect.com/science/article/pii/S0038092X20307672.

[11] Rodolfo Dufo-López and José L. Bernal-Agustín. Techno-economic analysis of grid-connected battery storage. *Energy Conversion and Management*, 91:394–404, 2015. ISSN 0196-8904. doi: https://doi.org/10.1016/j.enconman.2014.12.038. URL https://www.sciencedirect.com/science/article/pii/S0196890414010772.

[12] Energy-Charts. Energy-charts api 1.4, 2025. URL https://api.energy-charts.info/.

[13] eurostat. Electricity prices for household consumers - bi-annual data (from 2007 onwards), 2024. URL https://ec.europa.eu/eurostat/databrowser/view/nrg_pc_204/default/bar?lang=en.

[14] Bundesverband für Energie-und Wasserwirtschaft e.V. Standardlastprofile strom, 2025. URL https://www.bdew.de/media/documents/1999_Repraesentative-VDEW-Lastprofile.pdf.

[15] Fraunhofer Institut für Solare Energiesysteme ISE. Photovoltaics report, 2024. URL https://www.ise.fraunhofer.de/content/dam/ise/de/documents/publications/studies/Photovoltaics-Report.pdf.

[16] Bundesministerium für Umweltschutz Naturschutz nukleare Sicherheit und Verbraucherschutz. Kohleausstieggesetz, 2023. URL https://www.bmuv.de/faqs/kohleausstiegsgesetz.

[17] Bundesministerium für Wirtschaft und Klimaschutz. Gesetz zur Änderung des energiewirtschaftsrechts zur vermeidung von temporären erzeugungsüberschüssen, 2025. URL https://www.recht.bund.de/bgbl/1/2025/51/VO.html.

[18] BHKW Infozentrum GbR. Negative strompreise – fakten und statistiken, 2025. URL https://www.bhkw-infozentrum.de/wirtschaftlichkeit-bhkw-kwk/negative-strompreise-fakten-und-statistiken.html.

[19] Wilfried Hennings, Peter Stenzel, and Noah Pflugradt. Performance of a photovoltaic plus battery home system with load profile scenarios changing over the system life. *Energy Procedia*, 142:3252–3257, 2017. ISSN 1876-6102. doi: https://doi.org/10.1016/j.egypro.2017.12.499. URL https://www.sciencedirect.com/

science/article/pii/S1876610217362549. Proceedings of the 9th International Conference on Applied Energy.

[20] Mengjin Hu, Zhao Liu, Yaohuan Huang, Mengju Wei, and Bo Yuan. Estimation of rooftop solar photovoltaic potential based on high-resolution images and digital surface models. *Buildings*, 13(11):2686, 2023.

[21] IEA. Iea solar pv, 2024. URL https://www.iea.org/energy-system/renewables/solar-pv.

[22] Salvador Izquierdo, Marcos Rodrigues, and Norberto Fueyo. A method for estimating the geographical distribution of the available roof surface area for large-scale photovoltaic energy-potential evaluations. *Solar Energy*, 82 (10):929–939, 2008. ISSN 0038-092X. doi: https://doi.org/10.1016/j.solener.2008.03.007. URL https://www.sciencedirect.com/science/article/pii/S0038092X08000625.

[23] Iflah Javeed, Rahmat Khezri, Amin Mahmoudi, Amirmehdi Yazdani, and GM Shafiullah. Optimal sizing of rooftop pv and battery storage for grid-connected houses considering flat and time-of-use electricity rates. *Energies*, 14(12):3520, 2021.

[24] Samuel C. Johnson, Joshua D. Rhodes, and Michael E. Webber. Understanding the impact of non-synchronous wind and solar generation on grid stability and identifying mitigation pathways. *Applied Energy*, 262:114492, 2020. ISSN 0306-2619. doi: https://doi.org/10.1016/j.apenergy.2020.114492. URL https://www.sciencedirect.com/science/article/pii/S0306261920300040.

[25] Izabela Jonek-Kowalska and Wieslaw Grebski. Autarky and the promotion of photovoltaics for sustainable energy development: Prosumer attitudes and choices. *Energies*, 17(16), 2024. ISSN 1996-1073. doi: 10.3390/en17163919. URL https://www.mdpi.com/1996-1073/17/16/3919.

[26] Sebastian Krapf, Lukas Bogenrieder, Fabian Netzler, Georg Balke, and Markus Lienkamp. Rid—roof information dataset for computer vision-based photovoltaic potential assessment. *Remote Sensing*, 14(10), 2022. ISSN 2072-4292. doi: 10.3390/rs14102299. URL https://www.mdpi.com/2072-4292/14/10/2299.

[27] Tobias Kraschewski, Tim Brauner, Maximilian Heumann, and Michael H. Breitner. Disentangle the price dispersion of residential solar photovoltaic systems: Evidence from germany. *Energy Economics*, 121:106649, 2023. ISSN 0140-9883. doi: https://doi.org/10.1016/j.eneco.2023.106649. URL https://www.sciencedirect.com/science/article/pii/S0140988323001470.

[28] Haozhan Ni, Daoyang Wang, Wenzhuo Zhao, Wolin Jiang, E. Mingze, Chenyu Huang, and Jiawei Yao. Enhancing rooftop solar energy potential evaluation in

high-density cities: A deep learning and gis based approach. *Energy and Buildings*, 309:113743, 2024. ISSN 0378-7788. doi: https://doi.org/10.1016/j.enbuild.2023.113743. URL https://www.sciencedirect.com/science/article/pii/S0378778823009738.

[29] Xincheng Pan, Rahmat Khezri, Amin Mahmoudi, Amirmehdi Yazdani, and GM Shafiullah. Energy management systems for grid-connected houses with solar pv and battery by considering flat and time-of-use electricity rates. *Energies*, 14 (16):5028, 2021.

[30] Mathaios Panteli and Pierluigi Mancarella. Influence of extreme weather and climate change on the resilience of power systems: Impacts and possible mitigation strategies. *Electric Power Systems Research*, 127:259–270, 2015. ISSN 0378-7796. doi: https://doi.org/10.1016/j.epsr.2015.06.012. URL https://www.sciencedirect.com/science/article/pii/S037877961500187X.

[31] Sergio B Sepúlveda-Mora and Steven Hegedus. Making the case for time-of-use electric rates to boost the value of battery storage in commercial buildings with grid connected pv systems. *Energy*, 218:119447, 2021.

[32] Jørn Stene. Residential co2 heat pump system for combined space heating and hot water heating. *International Journal of Refrigeration*, 28(8):1259–1265, 2005. ISSN 0140-7007. doi: https://doi.org/10.1016/j.ijrefrig.2005.07.006. URL https://www.sciencedirect.com/science/article/pii/S0140700705001775. CO2 as Working Fluid - Theory and Applications.

[33] Peter Stenzel, Jochen Linssen, and Johannes Fleer. Impact of different load profiles on cost optimal system designs for battery supported pv systems. *Energy Procedia*, 75:1862–1868, 2015. ISSN 1876-6102. doi: https://doi.org/10.1016/j.egypro.2015.07.165. URL https://www.sciencedirect.com/science/article/pii/S1876610215009339. Clean, Efficient and Affordable Energy for a Sustainable Future: The 7th International Conference on Applied Energy (ICAE2015).

[34] Tibber. Strompreise, 2025. URL https://tibber.com/de/strompreise.

[35] Qing Zhong and Daoqin Tong. Spatial layout optimization for solar photovoltaic (pv) panel installation. *Renewable Energy*, 150:1–11, 2020. ISSN 0960-1481. doi: https://doi.org/10.1016/j.renene.2019.12.099. URL https://www.sciencedirect.com/science/article/pii/S0960148119319718.

[36] Qing Zhong, Jake R. Nelson, Daoqin Tong, and Tony H. Grubesic. A spatial optimization approach to increase the accuracy of rooftop solar energy assessments. *Applied Energy*, 316:119128, 2022. ISSN 0306-2619. doi: https://doi.org/10.1016/j.apenergy.2022.119128. URL https://www.sciencedirect.com/science/article/pii/S0306261922005062.

A. Appendix

Fire protection regulations in Germany 2024

Federal state	flammable modules (in m)	Non-flammable modules (in m)	Firewall (in m)
Baden-Württemberg	0	0	0
Bayern	0.5	0.5	0
Berlin	0.5	0.5	0
Brandenburg	0.5	0.5	0
Bremen	0	0.5	0
Hamburg	0.5	0.5	0
Hessen	0.5	0	0
Mecklenburg-Vorpommern	1.25	1.25	0
Niedersachen	0.5	0.5	0
Nordrhein-Westfalen	0	0	0
Rheinland-Pfalz	0.5	0.5	0
Saarland	1.25	1.25	0
Sachsen	1.25	0.3	0
Sachsen-Anhalt	0.5	0.5	0
Schleswig-Holstein	0.5	0	0
Thüringen	1.25	1.25	0

Case study one data

Algorithm	Cell size [m]	Time [ms]	Panel count	Power generated [kWh]
Greedy meta-heuristic	0.1	609	70	20193
	0.05	8640	77	22162
	0.025	137809	77	22158
Vertical	0.1	599	55	15842
	0.05	8658	72	20784
	0.025	132207	72	20784
Horizontal	0.1	609	66	19049
	0.05	8379	68	19632
	0.025	134306	68	19631
HorizontalSym	0.1	659	62	17907
	0.05	8504	66	19057
	0.025	126689	66	19055
VerticalSym	0.1	600	51	14694
	0.05	8411	70	20207
	0.025	125594	70	20204
IP	0.1	58175	76	21934

Case study two data

Algorithm	Cell size [m]	Time [ms]	Panel count	Power generated [kWh]
Greedy meta-heuristic	0.1	393	45	13404
	0.05	4148	50	14816
	0.025	57993	50	14818
Vertical	0.1	453	38	11407
	0.05	4275	44	13039
	0.025	59100	44	13042
Horizontal	0.1	433	43	12812
	0.05	4361	43	12812
	0.025	59215	43	12820
HorizontalSym	0.1	433	40	11701
	0.05	4356	40	11704
	0.025	60083	40	11708
VerticalSym	0.1	357	31	9403
	0.05	4432	36	10660
	0.025	60913	36	10670
IP	0.1	347732	47	13869